การสังเคราะห์อนุพันธ์เคอร์คิวมินเพื่อเป็นสารต้านเนื้องอก

นางสาวกิตติมา ชนเดชชาติวุฒิ

วิทยานิพนธ์นี้เป็นส่วนหนึ่งของการศึกษาตามหลักสูตรปริญญาวิทยาศาสตรมหาบัณฑิต
สาขาวิชาเคมี ภาควิชาเคมี
คณะวิทยาศาสตร์ จุฬาลงกรณ์มหาวิทยาลัย
ปีการศึกษา 2554

SYNTHESIS OF CURCUMIN DERIVATIVES AS ANTI-TUMOR AGENTS

Miss Kittima Chondejchartwut

A Thesis Submitted in Partial Fulfillment of the Requirements
for the Degree of Master of Science Program in Chemistry
Department of Chemistry
Faculty of Science
Chulalongkorn University
Academic Year 2011

Thesis title	SYNTHESIS OF CURCUMIN DERIVATIVES AS ANTI-TUMOR AGENTS
By	Miss. Kittima Chondejchartwut
Field of Study	Chemistry
Thesis Advisor	Associate Professor Supason Wanichwecharungruang, Ph.D.
Thesis Co-advisor	Assistant Professor Sumrit Wacharasindhu, Ph.D.

Accepted by the Faculty of Science, Chulalongkorn University in Partial Fulfillment of the Requirements for the Master's Degree

……..Dean of the Faculty of Science
(Professor Supot Hannongbua, Dr.rer.nat.)

THESIS COMMITEE

.....Chairman
(Assistant Professor Warinthorn Chavasiri, Ph.D.)

.....Thesis Advisor
(Associate Professor Supason Wanichwecharungruang, Ph.D.)

……. Thesis Co-advisor
(Assistant Professor Sumrit Wacharasindhu, Ph.D.)

……..Examiner
(Associate Professor Polkit Sangvanich, Ph.D.)

……..External Examiner
(Kriengsak Lirdprapamongkol, Ph.D.)

กิตติมา ชนเดชชาติวุฒิ : การสังเคราะห์อนุพันธ์เคอร์คิวมินเพื่อเป็นสารต้านเนื้องอก (SYNTHESIS OF CURCUMIN DERIVATIVES AS ANTI-TUMOR AGENTS) อ. ที่ปรึกษาวิทยานิพนธ์หลัก : รศ.ดร.ศุภศร วนิชเวชารุ่งเรือง,อ. ที่ปรึกษาวิทยานิพนธ์ร่วม ผศ.ดร. สัมฤทธิ์ วัชรสินธุ์ 59 หน้า.

ในงานวิจัยนี้ศึกษาเกี่ยวกับระบบนำส่งยาที่มีการออกฤทธิ์เสริมกันระหว่างพาหะนำส่งยาและตัวยาที่กักเก็บภายในเคอร์คิวมินและแพคลิแทกเซลมีการออกฤทธิ์เสริมกันในการฆ่าเซลล์มะเร็ง ดังนั้นจึงได้สร้างพาหะนำส่งยาที่มีเคอร์คิวมินเป็นโครงสร้างหลักและกักเก็บยาแพคลิแทกเซลไว้ภายใน อนุพันธ์ของเคอร์คิวมินสามารถสังเคราะห์ได้จากการติดสายพอลีเอทิลีนออกไซด์และสายปาล์มิเตตเข้าไปที่หมู่ไฮดรอกซีทั้งสองข้างของเคอร์คิวมินโดยอนุพันธ์ของเคอร์คิวมินที่ได้สามารถจัดเรียงตัวเป็นอนุภาคระดับไมโครได้เองในน้ำและแสดงฤทธิ์ต้านมะเร็งได้ดีกว่าเคอร์คิวมินอิสระ การเข้าสู่เซลล์ของอนุภาคสามารถศึกษาได้จากการใช้กล้องคอนฟอคอลฟลูออเรสเซ้นท์ไมโครสโคป เมื่อกักเก็บยาแพคลิแทกเซลภายในอนุภาคส่งผลให้มีฤทธิ์ต้านมะเร็งที่สูงขึ้นทั้งในเซลล์มะเร็งปกติและเซลล์มะเร็งที่ดื้อยาแพคลิแทกเซลเมื่อทำการทดลองเทียบกับยาแพคลิแทกเซลอิสระ

ภาควิชา……เคมี…… ลายมือชื่อนิสิต……..
สาขาวิชา…..เคมี…….…….. ลายมือชื่อ อ.ที่ปรึกษาวิทยานิพนธ์หลัก.....
ปีการศึกษา.. 2554……. ลายมือชื่อ อ.ที่ปรึกษาวิทยานิพนธ์ร่วม……

5272225323 : MAJOR CHEMISTRY
KEYWORDS : CURCUMIN / DRUGDELIVERY SYSTEM / MICELLES / PACLITAXEL / CANCER

KITTIMA CHONDEJCHARTWUT : SYNTHESIS OF CURCUMIN DERIVATIVES AS ANTI-TUMOR AGENTS. ADVISOR : ASSOC. PROF. SUPASON WANICHWECHARUNGRUANG, Ph.D., ASST. PROF. SUMRIT WACHARASINDHU, Ph.D., 59 pp.

Curcumin is a natural phenolic compound with diverse pharmacological activities and shows synergism effect with paclitaxel in killing cancer cells. However, the compound's low aqueous solubility and instability in physiological conditions have limited its application. Here water dispersible methoxy poly (ethylene oxide)-palmitate-curcumin conjugate (mPEO-CUR-PA) was synthesized by reacting curcumin with palmitic anhydride to give palmitoyl curcumin(CUR-PA), followed by coupling and coupling with methoxypoly (ethylene oxide) acetic acid (mPEO-COOH) obtained *via* succinylation of methoxypoly(ethylene oxide). The products could automatically self-assemble into water dispersible microspheres which by themselves showed better anti-tumor activity than free curcumin. The endocytosis of the microspheres into cancer cells was witnessed by confocal laser fluorescent microscope. Paclitaxel could be loaded into the obtained microspheres, and the paclitaxel-loaded mPEO-CUR-PA showed the increasing of anti-tumor activity in both the wild type and the paclitaxel-resistant cancer cells when compared to the activity of free paclitaxel.

Department : CHEMISTRY	Student's Signature .....
Field of Study : CHEMISTRY	Advisor's Signature .....
Academic Year : 2011	Co-advisor's Signature .....

ACKNOWLEDGEMENTS

First of all, I would like to express my sincere appreciation to my thesis advisor, Associate Professor Dr. Supason Wanichwecharungruang for her helpful supervision, invaluable assistance and generous encouragement to fulfill my achievement.

I would like to gratefully acknowledge my co-adviser, Assistant Professor Dr. Sumrit Wacharasindhu who not only firstly initiates this fascinating work but also pay a great attention, gives invaluable suggestion, extremely encourages and support me throughout this long work.

I also sincerely thank Assistant Professor Dr. Warinthorn Chavasiri, Associate Professor Dr. Polkit Sangvanich and Dr. Kriengsak Lirdprapamongkol for their time and suggestions as the committee members.

I gratefully appreciate to Miss Khajeelak Chiablaem, Dr. Kriengsak Lirdprapamongkol from Chulabhorn Research Institute for their advices, guidance and helps in cytotoxicity test. Very grateful thanks Associate Professor Dr. Sanong Ekgasit for light scattering and ATR-FTIR analysis.

I would not forget to thank Center for Petroleum, Petrochemicals and Advanced Materials and Graduate School, Chulalongkorn University for scholarship and financial support.

Last but not least, I would like to specially thank my family and my friends especially in Dr. Supason's Lab for their advice and encouragement throughout my master study.

CONTENTS

Page

Page

LIST OF TABLES

LIST OF FIGURES

Figure **Page**

LIST OF SCHEMES

LIST OF ABBREVIATIONS

DDS	Drug delivery systems
EPR	Enhanced Permeability and Retention
k	kio(s)
Da	Dalton
α	Alpha
β	Beta
κ	Kappa
mPEO	Methoxy poly(ethylene oxide)
PA	Palmitate
IC_{50}	The half maximal inhibitory concentration
μM	Micromolar
NPs	Nanoparticles
ALG	Alginate
CS	Chitosan
CUR	Curcumin
CURN	Curcumin nanoparticle
PVP	Polyvinylpyrrolidone
DPPH	di(phenyl)-(2,4,6-trinitrophenyl)iminoazanium
DCC	dicyclohexylcarbodiimide
DMAP	4-(N,N-dimethylamino)pyridine
MHz	Megahertz
PLGA	Poly (lactide-co-glycolide)
SMEDDS	Self-microemulsifying drug delivery system
δ	Chemical shift
°C	degree Celsius
g	gram (s)
Hz	hertz
h	hour
IR	Infrared

mg	milligram (s)
cm	centimeter (s)
mL	milliliter (s)
mV	millivolt
mW	milliwatt
min	minute (s)
MW	molecular weight
nm	nanometer (s)
NMR	nuclear magnetic resonance
DLS	Dynamic Light Scattering
ppm	parts per million
%	percent
cm^{-1}	per centimeter (s)
UV	Ultraviolet
FTIR	Fourier Transform Infarred Spectroscopy
cm^{-1}	unit of wavenumber (IR)
λ	wavelength
EtOAc	Ethyl acetate
TFA	Trifluoroacetic acid
MeOH	Methyl alcohol
CUR-PA	Palmitoyl curcumin
$CDCl_3$	Deuterated chloroform
Ar	Aromatic ring
MALDI-TOF	Matrix Assisted Laser Desorption Ionisation Ttime-Of-Flight mass spectrometer
m/z	mass to charge
DMF	Dimethyl formamide
mPEO-CUR-PA	Methoxy poly(etgylene oxide)- Curcumin-Palmitate conjugate
D_2O	Deuterium oxide
MWCO	Molecular weight cut off
CH_2Cl_2	Methylene chloride
J	Coulping constant

CMC	Critical micelle concentration
DMSO	Dimethyl sulfoxide
v/v	volume by volume
DIC	differential interference contrast
MTT	3-(4, 5-Dimethylthiazol-2-yl)-2,5-diphenyltetrazolium bromide
μL	Microliter

CHAPTER I

INTRODUCTION

1.1 Drug Delivery Systems

Many of the pharmacological properties of free drugs can be improved through the use of drug delivery systems (DDS). It offers numerous advantages compared to conventional dosage forms including improved efficacy, reduced toxicity, and improved patient compliance and convenience [1]. Drug carriers are substances that serve as mechanisms to improve the delivery and the effectiveness of drugs. Table 1.1 shows examples of problems exhibited by free drugs that can be improved by the use of drug delivery systems [2]. Various forms of carriers have been proposed ranging from conventional liposome, lipid-based carriers such as micelles, lipid emulsions, and lipid-drug complexes; also included are polymer-drug conjugates, polymer microspheres, polymeric micelles, polymeric vesicles, self-assembled polymer aggregates and porous inorganic particulates.

The desired effect of many medical treatments is usually obtained when the drug concentration is in the therapeutic range over a period of time. This is especially true for highly potent drugs, such as anti-cancer drugs. Administration of the entire drug dose at once using conventional pharmaceutical dosage will cause the overshoot drug concentration in the blood and results in high side effect. Depending on the therapeutic range and dose, the risk of toxic side effects can be dangerous. In contrast, because the human body eliminates active agents (drugs) automatically, thus drug concentration decreases over the time. With no proper DDS, the drug levels in the plasma that falls within the therapeutic range is attained for only a short time period.

DDS can control the release rate of drugs through various mechanism such as diffusion, erosion, and swelling. Therefore broad spectrums of release profiles have been reported. With appropriate DDS, a continuous drug supply can be provided as

replacement for the clearance of the drug from the human body, thus resulting in constant drug concentration at the site of action over a prolonged period.

Table1.1 Non-ideal properties of drugs and their therapeutic implications.

Problem	Implication	Effect of DDS
Poor solubility	A convenient pharmaceutical format is difficult to achieve, as hydrophobic drugs may precipitate in aqueous media. Toxicities are associated with the use of excipients sush as Cremphor (the solubilizer for paclitaxel in Taxol).	DDS sush as lipid micelles or liposomes provide both hydrophilic and hydrophobic environments, enhancing drug solubility.
Tissue damage on extravasation	Inadvertent extravasation of cytotoxic drugs leads to tissue damage, e.g., tissue necrosis with free doxorubicin.	Regulated drug release from the DDS can reduce or eliminate tissue damage on accidental extravasation.
Rapid breakdown of the drug *in vivo*	Loss of activity of the drug follows administration, e.g., loss of activity of camptothecins at physiological pH.	DDS protects the drug from premature degradation and functions as a sustained release system. Lower doses of drug are required.
Unfavorable pharmacokinetics	Drug is cleared too rapidly, by the kidney, for example, requiring high doses or continuous infusion.	DDS can substantially alter the pharmacokinetics of the drug and reduce clearance. Rapid renal clearance of small molecules is avoided.
Poor biodistribution	Drugs that have widespread distribution in the body can affect normal tissues, resulting in dose-limiting side effects, such as the cardiac toxicity of doxorubicin.	The particulate nature of DDS lowers the volume of distribution and helps to reduce side effects in sensitive, non-target tissues.
Lack of selectivity for target tissues	Distribution of the drug to normal tissues leads to side effects that restrict the amount of drug that can be administered. Low concentrations of drugs in target tissues will result in suboptimal therapeutic effects.	DDS can increase drug concentrations in diseased tissues such as tumors by the EPR effect. Ligand-mediated targeting of the DDS can further improve drug specificity.

1.1.1 Polymeric micelles

The polymeric micelles have been used widely in the delivery of various therapeutic drugs. Polymeric micelles are consisting of amphiphilic block copolymers. The amphiphilic polymer can self–assemble into core–shell architecture with hydrophobic center, in aqueous medium. The structure of a polymeric micelle is shown in Figure 1.1. These kinds of micelles are often used as drug carriers for controlled drug delivery systems [3-4]. The hydrophobic core of the polymeric micelle can trap hydrophobic drugs, while their hydrophilic shells make the micelle soluble and decrease the rate of clearance from the blood. In this way, with the use of DDS, poorly soluble drugs can be successfully solubilized in aqueous media.

From the fact that most carriers offer drug loading of less than 10%, and administration of large amount of carrier materials with no therapeutic function into the body is unavoidable. To improve this problem, carrier should be made to possess their own therapeutic function. This concept of bioactive carrier has been demonstrated earlier in a few works including the use of nano-vesicles constructed from pro-anticancer drug molecules to deliver another anti-cancer agent to cancer cells [5], and the use of UV absorptive carrier in the form of organic polymeric nanoparticles or hybrid organic-inorganic nanospheres for topical delivery of bioactive agent while at the same time the carriers act as sunscreening agents to protect both skin and the loaded drugs from UV radiation [6-7]. This work also involves the fabrication of bioactive carriers.

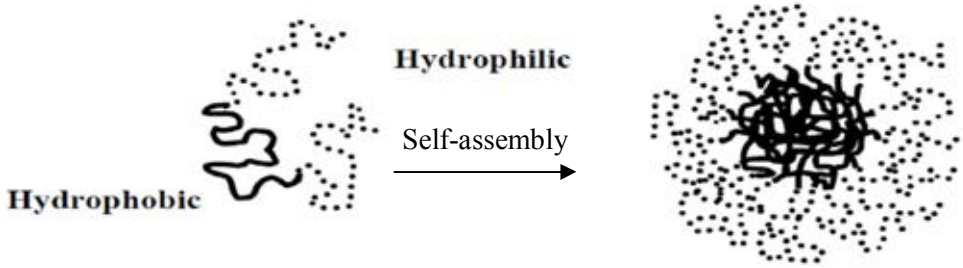

Figure1.1 Self-assembly of amphiphillic block polymer to form micelles in aqueous media

1.1.2 Tumor and drug delivery system

At the tumor site, an enhancement of vascular permeability critically affects tumor growth by facilitating an adequate supply of nutrients and possibly oxygen to meet the great demands of rapidly growing tumors. Tumor vascular permeability is important not only in tumor biology but also in delivery of macromolecular anti-cancer agents [8-11]. The vessel characteristics govern the supply of macromolecular compounds such as plasma proteins and macromolecular drugs as well as lipidic microparticles to the tumor tissues. Furthermore, the impaired clearance of macromolecules and lipidic particles from the interstitial space of tumor tissue contributes to retention of those delivered materials in tumor for long periods [8-9, 12-15]. This phenomenon has been called the tumor-selective *e*nhanced *p*ermeability and *r*etention (EPR) effect of macromolecules and lipidic particles. This EPR effect can be observed with macromolecules having an apparent molecular size larger than 50 kDa which have long plasma half-lives [16]. Therefore, the use of delivery carrier for anti-cancer drug can help delivering the drug more effectively comparing to the use of small drug molecule in which EPR has no effect.

1.1.3 The advantages of using drug delivery system.

1. Particle size and surface characteristics of carriers can be easily manipulated to achieve both passive and active drug targeting after parenteral administration.

2. They help controlling and sustaining the release of drugs during the transportation and at the site of localization. DDS can also alter organ distribution of the drug and subsequent clearance of the drug.

3. Controlled release and carrier degradation characteristics can be readily modulated by the choice of matrix constituents. Drug loading is relatively high and drugs can be incorporated into the systems without any chemical reaction; this is an important factor for preserving the drug activity.

4. Site-specific targeting can be achieved by attaching targeting ligands to surface of particles or use of magnetic guidance.

5. The system can be used for various routes of administration including oral, nasal, parenteral, intra-ocular etc.

1.2 Curcumin

Curcumin [1,7-bis(4-hydroxy-3-methoxyphenyl)-1, 6-heptadiene-3, 5-dione] is the polyphenol active ingredient derived from the rhizome of turmeric (*Curcuma longa*) (Figure 1.1). The powdered turmeric has been used in Asian cookery, medicine, cosmetics and fabric dying for more than twenty centuries. This compound has a long history of use in traditional medicines of Thai, India and China. In food and manufacturing, curcumin is currently used in perfumes and as a natural yellow coloring agent, as well as an approved food additive to flavor various types of curries and mustards. Recent emphasis on the use of natural and complementary medicines in Western medicine has drawn the attention of the scientific community to this ancient remedy. Research has revealed that curcumin has a surprisingly wide range of beneficial properties, including anti-inflammatory, antioxidant, chemopreventive and chemotherapeutic activity. These activities have been demonstrated both in cultured cells and in animal models and have paved the way for ongoing human clinical trials [17].

Figure1.2 *Curcuma longa*

Turmeric was isolated and structurally characterized. The yellow-pigmented fraction of Curcuma longa contains curcuminoids. The major curcuminoids present in turmeric are curcumin, demethoxycurcumin and bisdemethoxycurcumin. Commercial curcumin contains curcumin (~77%), demethoxycurcumin (~17%), and bisdemethoxycurcumin (~3%) as its major components (Figure 1.3).

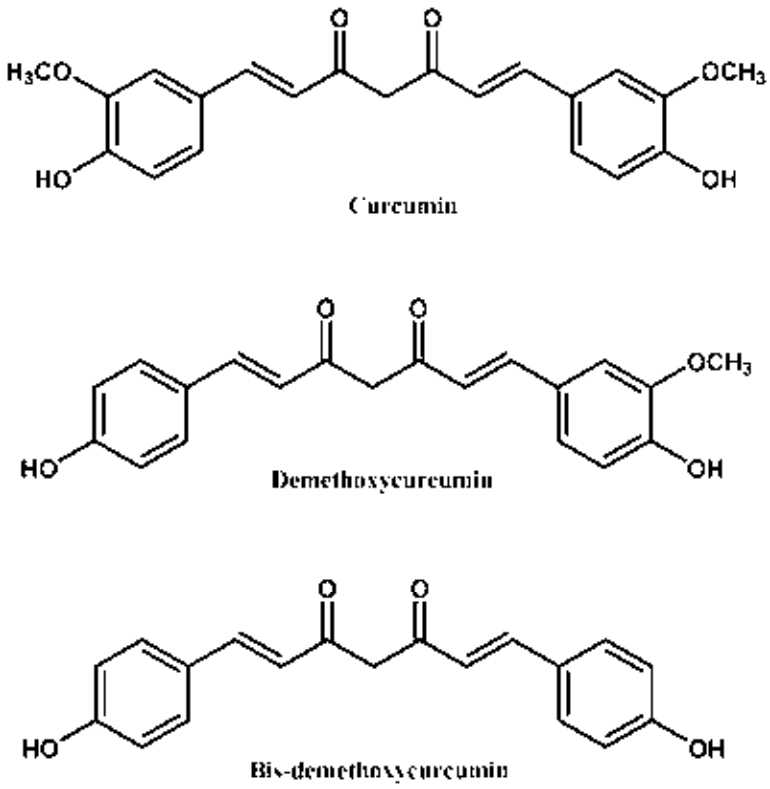

Figure1.3 Structure of curcumin, demethoxycurcumin and bis-demethyoxycurcumin

Chemically, curcumin is insoluble in water but is quite soluble in organic solvents such as dimethyl sulfoxide, ethanol, methanol, or acetone and has a melting point of 183^{o}C, molecular formula of $C_{21}H_{20}O_6$, and molecular weight of 368.37 g/mol. Spectrophotometrically, curcumin has a maximum absorption (λ_{max}) in methanol at 430 nm [18]. It absorbs maximally at 415 to 420 nm in acetone, and a 1% solution of curcumin has 1650 absorbance units. Curcumin has a brilliant yellow hue at pH 2.5 to 7 and takes on a red hue at pH >7. Curcumin is a bis-α,β-unsaturated β-

diketone (commonly called diferuloylmethane), which exhibits keto–enol tautomerism having a predominant keto form (Figure1.4). Curcumin is stable at acidic pH but is unstable at neutral and basic pH. The stability of curcumin and its chemical degradation has been investigated by several laboratories with varying results. [19] This natural pigment molecule decomposes very rapidly, giving out vanillin, ferulic acid, feruloylmethane and trans-6-(4-hydroxy-3-methoxyphenyl)-2,4-dioxo-5-hexenal as its degradation products (Figure 1.5) [19]. Amongst the three major compounds, bis-demethoxycurcumin is the most stable, while curcumin is the fastest decomposed and photounstable compound [20]. Pure turmeric was found to have the highest concentration of curcumin with an average of 3.14% by weight, while curry powders contained relatively low amounts of curcumin. In addition, curcumin itself exists in several forms that exhibit different potencies as antioxidants and anti-tumor agents. Thus, the actual amount of curcumin used in various studies is often unclear [17].

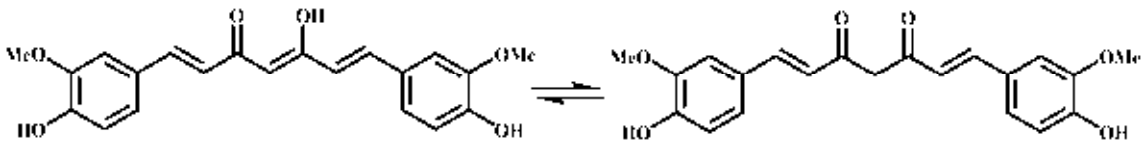

Figure1.4 Curcumin keto-enol tautomerism

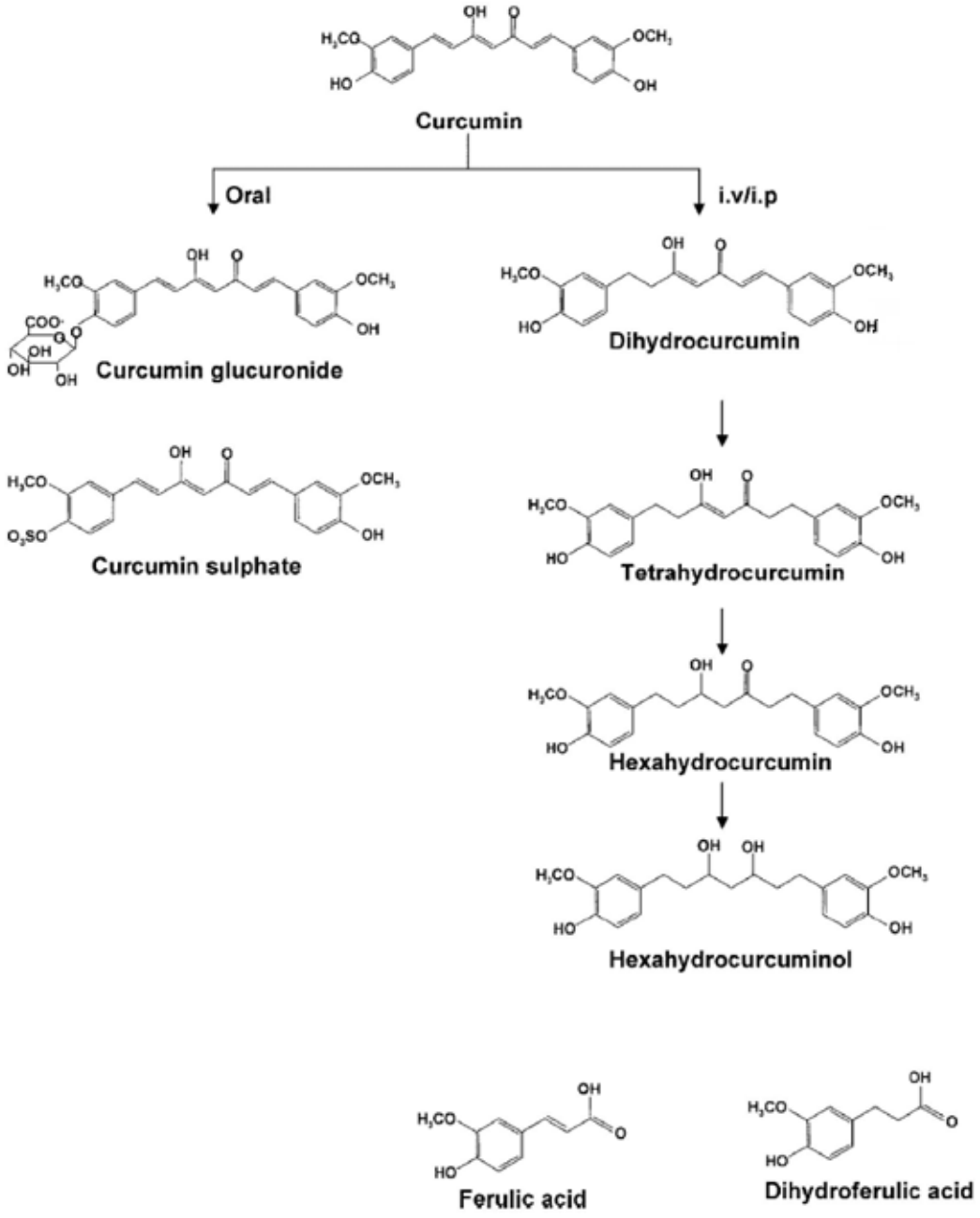

Figure1.5 Structure of curcumin and its metabolites

Curcumin is not toxic to animals or humans even at high doses [21]. For centuries, curcumin has been consumed as a dietary spice at doses up to 100 mg/day. Clinical trials phase I indicate that human beings can tolerate a dose as high as 8 g/day with no side effects [21]. Consonant with preclinical demonstrations of curcumin's anti-inflammatory and anti-cancer properties, disease targets include neoplastic and

preneoplastic diseases such as multiple myeloma, pancreatic cancer, myelodysplastic syndromes, and colon cancer [22], and conditions linked to inflammation such as psoriasis, and Alzheimer's disease [23].Curcumin and its disease targets are schematically shown in Figure 1.6 [20]. The desirable preventive or putative therapeutic properties of curcumin have been considered to be associated with its antioxidant [24] and anti-inflammatory properties [25-26]. Curcumin has been shown to be effective in acute as well as chronic models of inflammation.

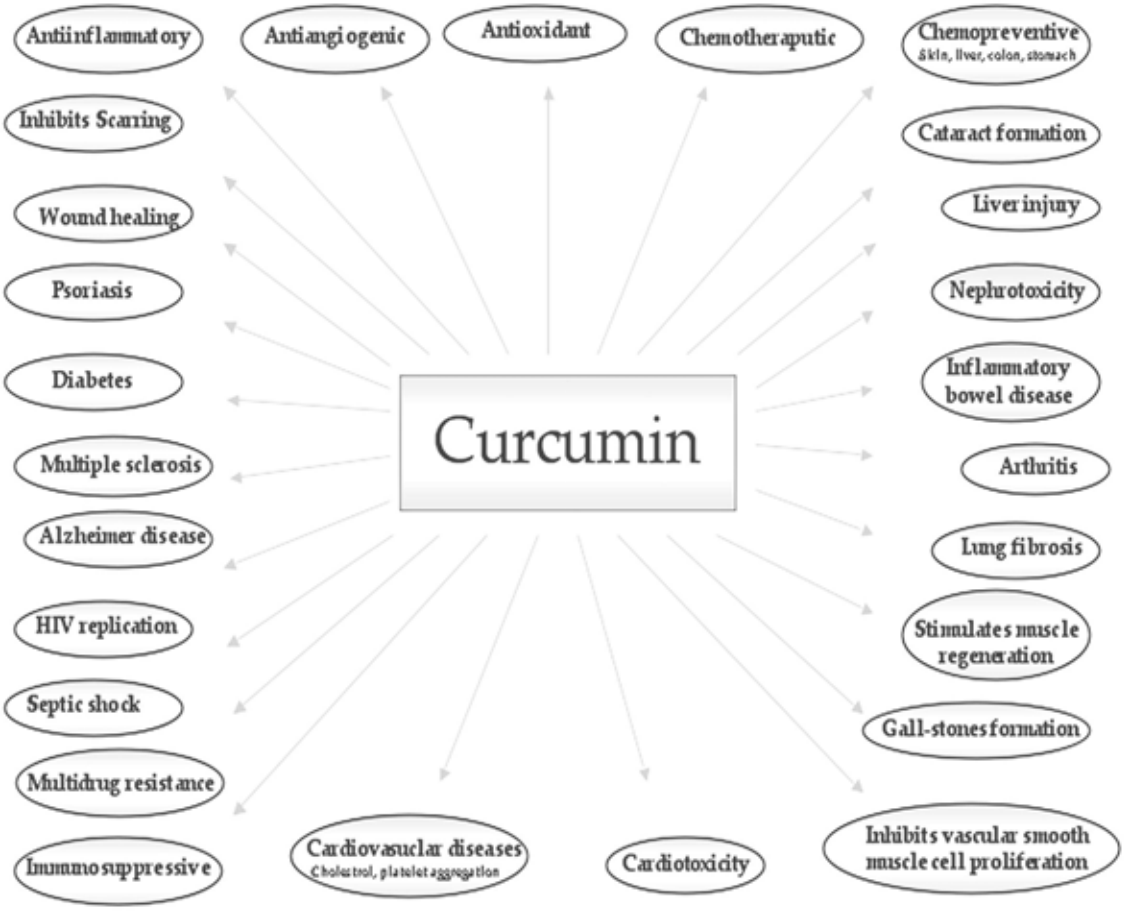

Figure1.6 Disease targets of curcumin [20]

Various studies have shown that curcumin modulates numerous targets (Figure 1.7). These include the growth factors, growth factor receptors, transcription factors, cytokines, enzymes, and genes regulating apoptosis [20].

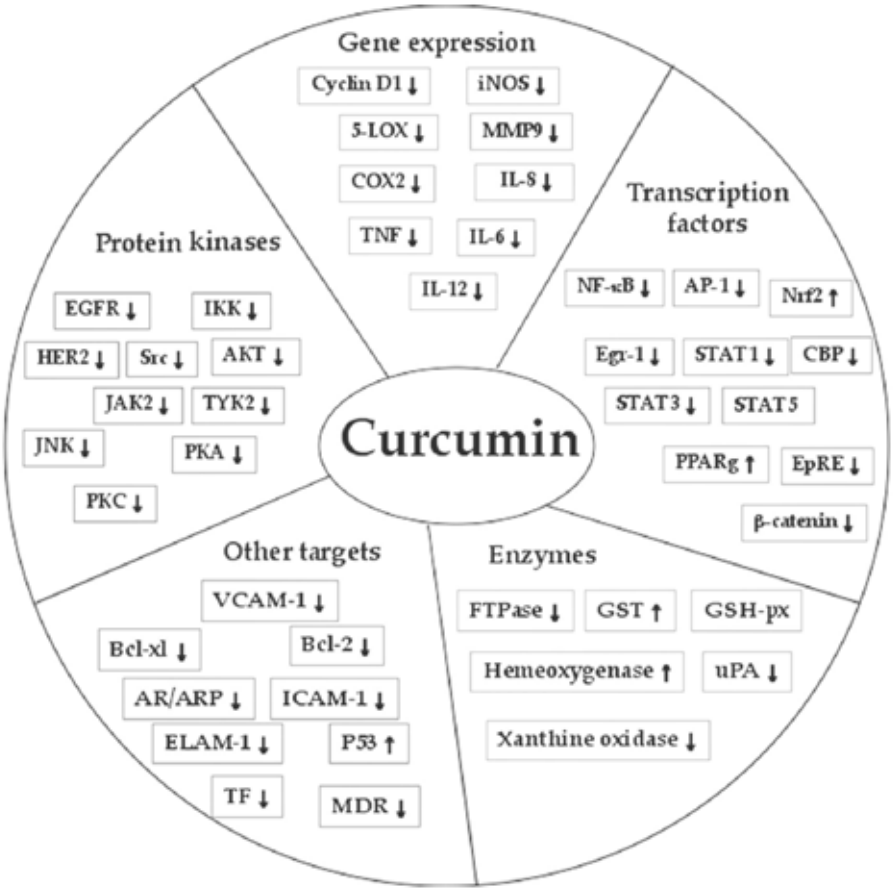

Figure1.7 Molecular targets of curcumin [20]

Furthermore, curcumin can reverse drug resistance in cancer cells by down-regulating expression levels of P-gp, MRP-1 and ABCG2, which are three major ABC drug transporters responsible for increased drug efflux in multidrug resistant cancer cells [27-28]. The compound has been shown to be able to improve the therapeutic outcome of paclitaxel treatment by suppressing activation of NF-κB and Akt survival signals induced by paclitaxel [29-30]. Aggarwal's group has demonstrated that curcumin can suppress paclitaxel-induced expression of NF-κB–regulated gene

products and prevent breast cancer metastasis to the lung in nude mice [31-32]. Thus the use of paclitaxel-curcumin combination is a promising way to kill cancer cells more effectively [33].

However, curcumin is unstable, possesses poor absorption, high rate of metabolism andrapid elimination from the body. Numerous approaches have been undertaken to improve the bioavailability of curcumin. These approaches involve, (i) the use of adjuvant like piperine that interferes with glucuronidation; (ii) the use of liposomal curcumin; (iii) curcumin nanoparticles; (iv) the use of curcumin phospholipid complex; and (v) the use of structural analogues of curcumin. Modulation of route and medium of curcumin administration, blocking of metabolic pathways by concomitant administration with other agents, and structural modification of curcumin are the main strategies now being explored in attempts to improve the bioavailability of curcumin. Attempts at enhanced *in vitro* and *in vivo* efficacies of curcumin through the use of DDS such as nanoparticles, liposomes, and defined phospholipid complexes offer significant promise as they appear to provide longer circulation, better permeability and resistance to metabolic processes [19].

1.3 Literature reviews

1.3.1 Curcumin encapsulated

In 2007, Aziz *et al*. reduced the color staining effect and enhanced the stability of curcumin via microencapsulation using gelatin coacervation method. Ethanol and acetone were used as coacervating solvents. Microencapsulation resolved the color-staining problem and enhanced the flow properties and photo-stability of curcumin. Nevertheless, it was found that acetone gave more spherical curcumin microcapsules with higher yield, higher curcumin loading, and higher entrapment efficiency comparing to ethanol. The in vitro release of curcumin after microencapsulation was slightly prolonged [34].

In 2007, Bisht *et al*. synthesized polymeric nanoparticle encapsulated with curcumin (nanocurcumin) utilizing the micellar aggregates of cross-linked and random copolymers of N-isopropylacrylamide with N-vinyl-2-pyrrolidone and poly(ethyleneglycol) monoacrylate. The obtained nanocurcumin showed the size distribution in the 50 nm range, and was readily dispersible in aqueous media. Nanocurcumin demonstrated comparable in vitro therapeutic efficacy to free curcumin against a panel of human pancreatic cancer cell lines, as assessed by cell viability and clonogenicity assays in soft agar. Further, nanocurcumin's mechanisms of action on pancreatic cancer cells mirrored that of free curcumin, including induction of cellular apoptosis, blockade of nuclear factor kappa B activation, and down regulation of steady state levels of multiple proinflammatory cytokines [35].

In 2008, Abhishek *et al*. synthesized a novel polymeric amphiphile, mPEO–PA, with methoxy poly(ethylene oxide) (mPEO) as the hydrophilic and palmitic acid (PA) as the hydrophobic segment. mPEO–PA conjugate undergoes self-assembly in an aqueous environment. The micelles were spherical in shape, with a mean diameter of 41.43 nm. The utility of mPEO–PA to entrap curcumin in the core of nanocarrier was investigated. Drug-loaded micelle nanoparticles showed good stability in physiological condition (pH 7.4), in simulated gastric fluid (pH 1.2) and in simulated intestinal fluid (pH 6.8). This micellar formulation can be used as an enzyme-triggered drug release carrier, as suggested by in vitro enzyme-catalyzed drug release using pure lipase and HeLa cell lysate. The IC_{50} of free curcumin and encapsulated curcumin was found to be 14.32 and 15.58 μM, respectively [36].

In 2009, Jing Cui *et al*. developed self-microemulsifying drug delivery system (SMEDDS) to improve the solubility and oral absorption of curcumin. The optimal formulation of SMEDDS was comprised of 57.5% surfactant (emulsifier OP:Cremorphor EL = 1:1), 30.0% co-surfactant (PEO 400) and 12.5% oil (ethyl oleate). The solubility of curcumin (21 mg/g) was significantly increased in SMEDDS. The average particle size of SMEDDS-containing curcumin was about

21nm when diluted in water. The dissolution study *in vitro* showed that more than 95% of curcumin in SMEDDS could be dissolved in pH 1.2 or pH 6.8 buffer solutions in 20 min, however, less than 2% for crude curcumin was soluble in 60 min. The *in situ* absorption property of curcumin-loaded SMEDDS was evaluated in intestines of rats. The results showed that the absorption of curcumin in SMEDDS was *via* passive transfer by diffusion across the lipid membranes. The results of oral absorption experiment in mice showed that SMEDDS could significantly increase the oral absorption of curcumin compared with its suspension [37].

In 2009, Shaikh *et al*. encapsulated curcumin into poly (lactide-co-glycolide) (PLGA) nanoparticles by emulsion technique. The obtained nanoparticles were spherical in shape with particle size of 264 nm (polydispersity index 0.31) and 76.9% entrapment at 15% loading. X-Ray diffraction analysis revealed the amorphous nature of the encapsulated curcumin. The in vitro release was predominantly by diffusion phenomenon and followed Higuchi's release pattern. The *in vivo* pharmacokinetics revealed that curcumin entrapped nanoparticles demonstrate at least 9-fold increase in oral bioavailability when compared to curcumin administered with piperine as absorption enhancer [38].

In 2010, Das *et al*. prepared the composite nanoparticles (NPs) by three different carriers, polymers-alginate (ALG), chitosan (CS), and pluronic-by ionotropic pre-gelation followed by polycationic cross-linking. Pluronic F127 was used to enhance the solubility of curcumin in the ALG-CS NPs. The particles were nearly spherical in shape with an average size of 100 ± 20 nm. Encapsulation efficiency (%) of curcumin in composite NPs considerably increased over ALG-CS NPs without pluronic. The *in vitro* drug release profile along with release kinetics and mechanism from the composite NPs were studied under simulated physiological conditions for different incubation periods. A cytotoxicity assay showed that composite NPs at a concentration of 500 μg/mL were nontoxic to HeLa cells. Cellular internalization of curcumin-loaded composite NPs was confirmed from green fluorescence inside the

HeLa cells. The half-maximal inhibitory concentrations for free curcumin and encapsulated curcumin were found to be 13.28 and 14.34 μM, respectively [39].

In 2010, Anand *et al*. encapsulated curcumin in nanoparticulate formulation based on poly (lactide-co-glycolide) (PLGA) and a stabilizer polyethylene oxide (PEO)-5000 with 97.5% efficiency and particle diameter of 80.9 nm. Overall they demonstrated that curcumin-loaded PLGA nanoparticles formulation possessed enhanced cellular uptake, and increased *in vitro* bioactivity and superior bioavailability with longer in vivo half-life comparing to curcumin [40].

In 2010, Feng *et al*. developed a novel curcumin nanoparticle system (CURN) using nanoprecipitation technique with polyvinylpyrrolidone (PVP) as the hydrophilic carrier. The results indicated that CURN improved the physicochemical properties of CUR, including a reduction in particle size and the formation of an amorphous state with hydrogen bonding, both of which increased the drug release of the compound. Moreover, *in vitro* studies indicated that CURN significantly enhanced the antioxidant and antihepatoma activities of curcumin ($P < 0.05$). Consequently, they suggested that CURN could be used to reduce the dosage of curcumin and to improve its bioavailability, thus meritting further investigation for therapeutic applications [41].

1.3.2 Curcumin derivatives as a prodrug

In 2000, Kumar *et al*. synthesized di-O-glycinoyl curcumin (I), di-O-glycinoyl-C4-glycyl-curcumin (II), 5'-deoxy-5'-curcuminyl thymidine (5'-cur-T) (III) and 2'-deoxy-2'-curcuminyl uridine (2'-cur-U) (IV) and characterized th productsby elemental analysis & 1H NMR. The antibacterial activities of these four bioconjugates have been tested particularly for multi resistant micro-organisms. Best results are shown by I & IV. These bioconjugates served dual purpose of systemic delivery as well as therapeutic agents against viral diseases [42].

In 2003, Mohri *et al*. synthesized and characterized curcumin derivatives; monoglycosylcurcumin and diglycosylcurcumin (Figure 1.8). The presence of glycosyl groups was the cause of increasing water solubility of curcumin [43].

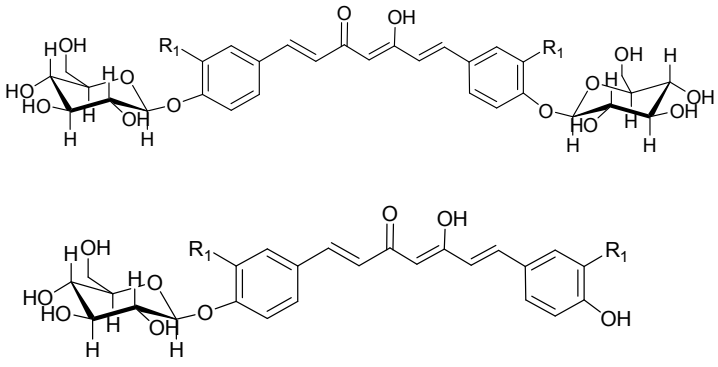

(R_1 = -OCH_3)

Figure1.8 Diglycosylcurcumin (upper) and Monoglycosylcurcumin (lower)

In 2005, Venkateswarlu *et al.* synthesized series of curcumin analogs through the condensation of appropriately protected hydroxybenzaldehydes with acetylacetone, followed by deprotection. The antioxidant activity of these analogs was determined by superoxide free radical nitroblue tetrazolium and DPPH free radical scavenging methods and the polyhydroxycurcuminoids displayed excellent antioxidant activity. These analogs showed cytotoxicity to lymphocytes and promising tumor-reducing activity on Dalton's lymphoma tumor cells [44].

In 2007, Safavy *et al*. conjugated of curcumin to two different sized poly(ethylene oxide) molecules in an attempt to overcome the low aqueous solubility of this natural product while retaining cytotoxic activity against human cancer cell lines. The soluble conjugates exhibited enhanced cytotoxicity as compared to that of the parent drug. The water-soluble conjugates may provide information useful for the development of injectable curcumin conjugates [45].

In 2010, Tang *et al*. synthesized series of backbone-type curcumin-derived polymers (Figure 1.9). The polymers possessed tailored curcumin-loading contents and water-solubility. The PCurc 8 was water soluble, i.v. injectable, and stable in physiological conditions. PCurc 8 was more cytotoxic to SKOV-3, MCF-7, and OVCAR-3 cancer cell lines than curcumin. The PCurc 8 arrested the SKOV-3 cell cycle at the G0/G1 phase *in vitro* and induced cell apoptosis partially through caspase-3 dependent pathway [46].

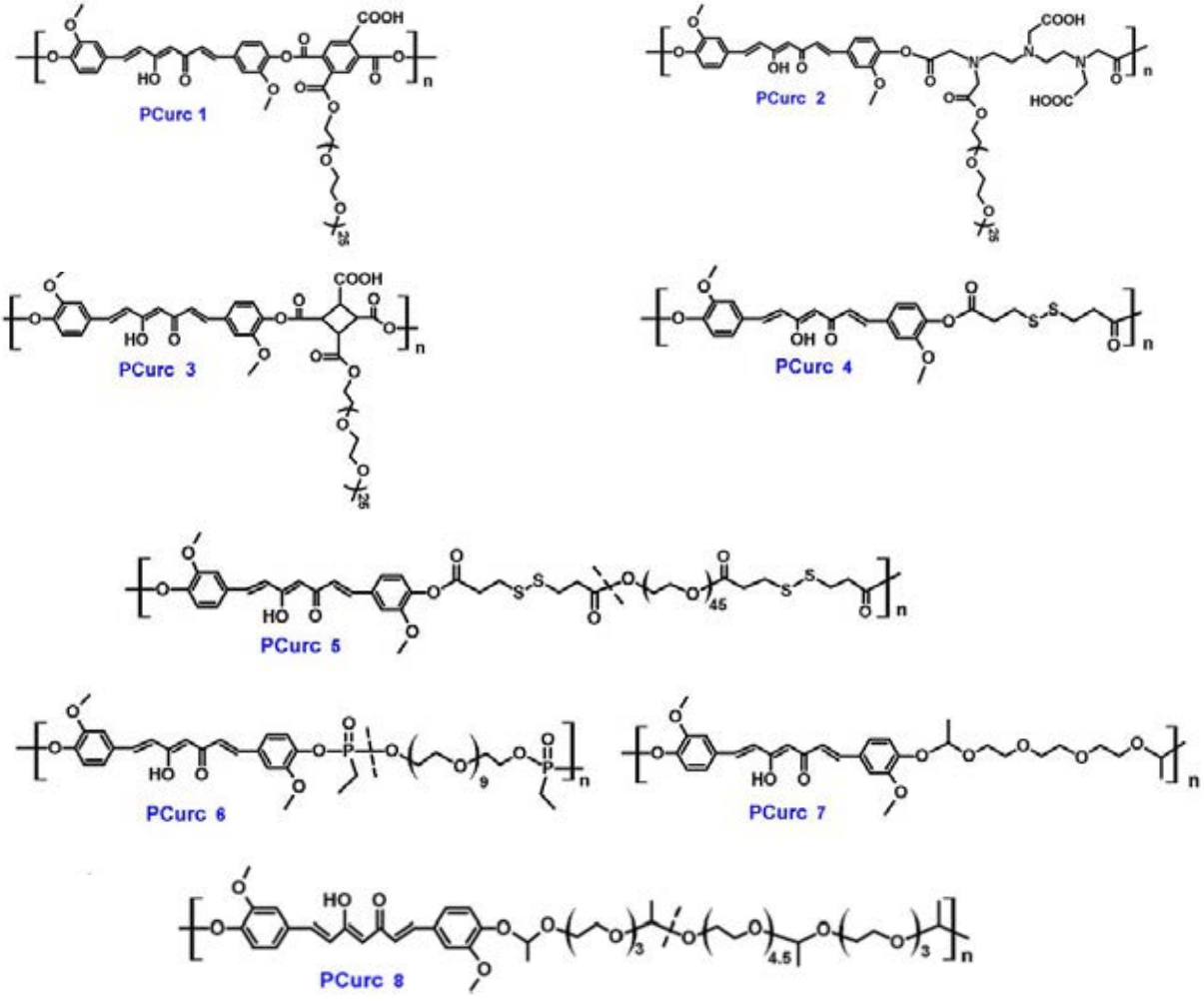

Figure1.9 Structure of series of backbone-type curcumin-derived high polymers

In 2011, Manju *et al*. synthesized curcumin conjugate with hyaluronic acid (Figure 1.10). The conjugate solubility in water was several folds higher comparing to

free curcumin. The conjugate formed micelles in aqueous media which stabilized the curcumin even in alkaline media in which free curcumin rapidly degraded. Conjugated curcumin also showed cytotoxicity reflecting its potential in targeted drug delivery applications [47].

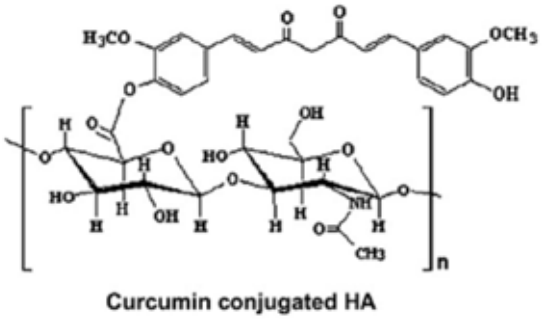

Figure1.10 Curcumin conjugated HA

1.3.3 Paclitaxel encapsulated

In 2004, Huh *et al*. synthesized amphiphilic block copolymers with poly(ethylene glycol)(PEG) as a hydrophilic block and various;PDENA, PPA or PLA as the hydrophobic moieties (Figure1.11). The amphiphillic polymer could self-assemble to form polymer micelles in aqueous media. Paclitaxel was loaded in to micelles. The hydrotropic polymer micelles exhibited a high drug loading capacity with enhanced long-term stability [48].

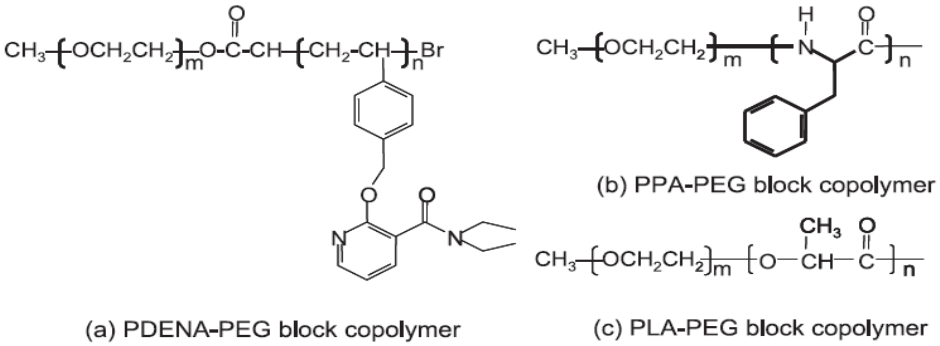

Figure1.11 Structure (a) PDENA-PEG block copolymer, (b) PPA-PEG block copolymer and (c) PLA-PEG block copolymer

In 2008, Mugabe *et al*. synthesized two different types of hydrophobically derivatized hyperbranched polyglycerols (dHPGs) (HPGC10-polyethylene glycol (PEG) and polyethyleneimine (PEI)-C18-HPG), paclitaxel was loaded into these nanospheres. In the PEI-C18- HPG formulation released only ≈ 40% of the initially incorporated paclitaxel while up to 80% was released from HPG-C10-PEG. Moreover, only paclitaxel/HPG-C10-PEG was stable in acidic urine. *In vitro*, all paclitaxel formulations potently decreased bladder cancer proliferation although paclitaxel/ HPG-C10-PEG was slightly less cytotoxic than standard Taxol. By contrast, *in vivo*, the mucoadhesive HPG-C10-PEG formulation of paclitaxel was significantly more effective in reducing orthotopic tumour growth than Taxol and was well tolerated [49].

1.3.4 Combination of curcumin and paclitaxel

In 2004, Bava *et al*. reported the mechanism-based evidence that curcumin sensitized tumor cells to be more efficiently responsive towards therapeutic effect of Taxol. They concluded that taxol and curcumin showed the synergism in the down-regulation of NF-kB and serine/threonine kinase Akt pathways. An electrophoretic mobility shift assay revealed that activation of NF-kB induced by Taxol was down-regulated by curcumin. They identified that curcumin-down-regulated Taxol induced phosphorylation of the serine/threonine kinase Akt, a survival signal which in many instances was regulated by NF-kB [50].

1.4 Rationale

Here we propose a novel bioactive carrier that not only possesses therapeutic function but also works synergistically with the loaded drug molecules, thus enabling;

1) An effective administration of the drugs into the cancer cells with no extra burden of non-therapeutic carrier materials for the body.

2) An improvement of the treatment from the therapeutic action of the carrier materials and an enhancement of drug action through the synergism between the carrier material and the loaded drug.

With this arrangement, the synergism of the two drugs can be maximized since the ratio of the two drugs delivered into the same cells at the same time can be more precisely controlled. As the administration of paclitaxel also requires proper drug carrier and as mentioned above that curcumin needs delivery technology for effective therapeutic result, therefore, here in this work we synthesize amphiphillic curcumin derivative and used the obtained derivative alone to construct carrier for paclitaxel delivery. Curcumin is nontoxic and usually is administered at much higher dose than paclitaxel, thus it is reasonable to make curcumin into carrier which is usually used in a greater amount comparing to the amount of the loaded drug (in this case paclitaxel). By incorporating paclitaxel into curcumin-carrier, the possibility that the two drugs will be delivered into the same cells at the same time is maximized and thus a full advantage of their synergistic action can be effectively harness. We will modify the curcumin structure (Figure 1.12) by attaching to it the polyethylene oxide moieties (to give hydrophilic and stealth character for good water dispersion with minimal blood clearance) and the palmitate moieties (to give hydrophobic character for stable micellar core with ability to hold hydrophobic paclitaxel), thus making the modified curcumin molecules amphiphilic and capable of assembling into water dispersible stealth micellar architectures.

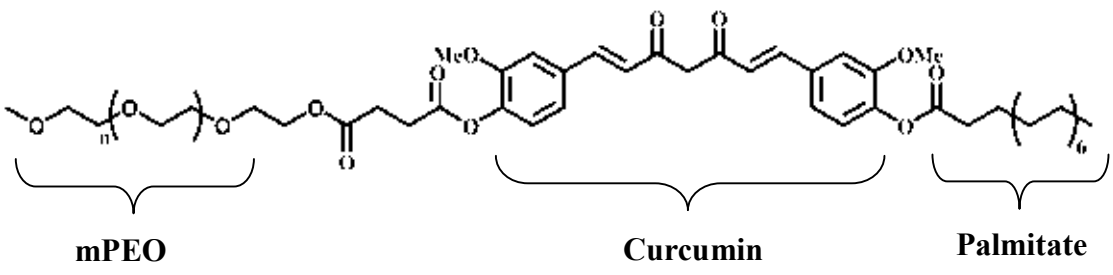

Figure1.12 Structure of target molecule; mPEO-CUR-PA

1.5 Research Objectives

The objectives of this research can be summarized as follows:

1. To synthesis poly(ethylene oxide) methyl ether-/palmitate(mPEO-CUR-PA)-grafted curcumin (mPEO-CUR-PA).
2. To characterize the mPEO-CUR-PA.
3. To prepare the micelles of mPEO-CUR-PA and encapsulate paclitaxel into the micelles.
4. To characterize the micelles of mPEO-CUR-PA and paclitaxel loaded micelles.
5. To study cytotoxicity of mPEO-CUR-PA and paclitaxel loaded micelles with S102, A549 and A549/RTeto cells.

CHAPTER II

EXPERIMENTAL

2.1 Materials

Curcumin (>98%), succinic anhydride were purchased from Acros organics (Geel, Belgium) while methoxy poly(ethylene oxide) (mPEO, Mn ≈ 750), plamitic anhydried (97%), dicyclohexylcarbodiimide (DCC), 4-(N,N-dimethylamino)pyridine(DMAP) and lipophillic Sephadex LH-20 were purchased from Aldrich (Steinheim, Germany). Silica gel 60 (0.063-0.200 nm) for column chromatography was purchased from Merck KGaA (Darmstadt, Germany). Triethylamine (Carlo Erba reagent, MI, Italy), pyridine (Carlo Erba) and dimethylformamide (RCI labscan, BKK, Thailand) were dry and triply distilled before use. All other chemicals were reagent grade and all solvents were triply distilled before use.

^{1}H-NMR spectrum was acquired at 400 MHz (Varian Company, USA) while UV-Visible absorption spectrum was taken at 200-600 nm using UV2500 spectrophotometer (Shimadzu Corporation, Kyoto, Japan) measuring in a quartz cell of 1 cm pathlength with thermostated at 25 ˚C. Infrared spectrum was obtained on germanium reflection element using a Nicolet 6700 ATR-FT-IR spectrometer (Thermo Electron Corporation, Madison, WI, USA). Mass spectrum was acquired on Microflex MALDI-TOF mass spectrometry (Bruker Daltonik GmbH, Germany), sinapinic acid was used as matrix and samples were prepared in a 50:50(v/v) mixture of 0.1% TFA/acetonitrile. Fluorescent images were acquired on Confocal Microscopes, Nikon Ti-E Inverted Microscope Confocal Nikon C1si-system (Nikon Corpopation, Tokyo, Japan).

2.2 Synthesis of palmitoylcurcumin (CUR-PA)

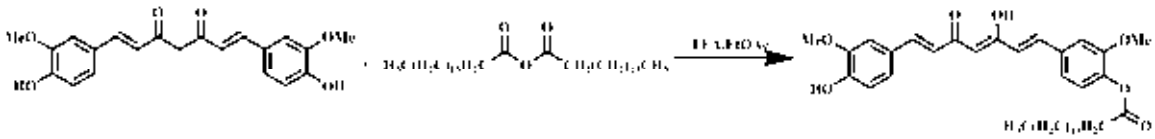

Scheme 2.1 Synthesis of palmitoylcurcumin.

The attachment of palmitoyl group to the hydroxyl moiety of curcumin was carried out by reacting curcumin with palmitic anhydride. Palmitic anhydride (0.5 g, 1.0 mmol) was added to a solution of curcumin (1.84 g, 5.0 mmol) in 100 ml of dry ethyl acetate (EtOAc). The mixture was stirred at 0 °C under nitrogen atmosphere for 15 min. Then triethylamine (0.7 ml, 5.0 mmol) was slowly added to the mixture, and stirring was continued at room temperature overnight. The solvent was evaporated and crude mixture was purified on silica gel column, using a 20-40% EtOAc gradient in hexane and reprecipitate in MeOH to obtained 52.28% yields of yellow powder. The product was characterized by ^{1}H-NMR, FT-IR, UV-visible absorption and MALDI-TOF spectroscopy.

Palmitoylcurcumin (CUR-PA): ^{1}H-NMR ($CDCl_3$, 400 MHz, δ,ppm) 7.60 (Ar-C**H**=CH-C=O-CH_2-C=O-CH=C**H**-Ar-, dd, J = 15.8, 1.9 Hz, 2H), 7.09 – 7.17 (m, 3H), 7.04 (d, J = 8.2 Hz, 2H), 6.93 (d, J = 8.2 Hz, 1H), 6.46 – 6.58 (Ar-CH=C**H**-C=O-CH_2-C=O-C**H**=CH-Ar-, m, 2H), 5.88 (-C=O-C**H**$_2$-C=O-, s, 1H), 5.83 (-C=O-C**H**$_2$-C=O-, s, 1H), 3.95 (C**H**$_3$-O-Ar-O-C=O-CH_2-CH_2-, s, 3H), 3.87 (C**H**$_3$-O-Ar-O-H, s, 3H), 2.58 (-Ar-O-C=O-C**H**$_2$-CH_2-, t, J = 7.5 Hz, 2H), 1.71 – 1.81 (-Ar-O-C=O-CH_2-C**H**$_2$-$(CH_2)_n$-, m, 2H), 1.21-1.46 (-Ar-O-C=O-CH_2-CH_2-(C**H**$_2$)$_n$-, m, 24H), 0.88 (-Ar-O-C=O-CH_2-CH_2-$(CH_2)_n$-OC**H**$_3$, t, J = 6.8 Hz, 3H); UV-visible spectroscopy (MeOH) λ_{max} at 412 nm; FT-IR (cm^{-1}) CH-stretching at 2914.02 and 2847.60, C=O stretching at 1754.98, C=C stretching at 1625.46, C=O streching keto-enol at 1585.61 and CH-bending at 1207.01and1123.08; MALDI-TOF (m/z) MW. 607.71.

2.3 Synthesis of methoxy poly(ethylene oxide) acetic acid (mPEG-COOH)

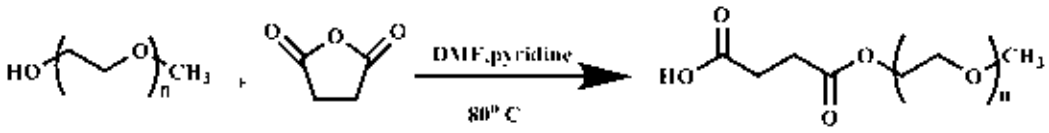

Scheme 2.2 Synthesis of methoxy poly(ethylene oxide) acetic acid.

Succinic anhydride (6.6 g, 66.6 mmol) was added to a solution of methoxy poly(ethylene oxide) (10 g, 13.3 mmol) in dry DMF. The mixture was stirred at 80 °C under nitrogen atmosphere for 30 min. Then pyridine was slowly added to the mixture, and stirring was continued at 80 °C for 3 days (Scheme 2.2). Succinic acid was eliminated by Sephadex column chromatography, using 100% MeOH to obtain 9.39% of mPEO-COOH. The product was characterized by ^{1}H-NMR, FT-IR and MALDI-TOF spectroscopy.

Poly(ethylene oxide) acetic acid (mPEG-COOH): ^{1}H-NMR (D_2O, 400 MHz,δ, ppm) 4.12 (CH_3O-CH_2-C**H$_2$**-(O-CH_2-CH_2)$_n$-, s, 2H), 3.41 – 3.66 (CH_3O-CH_2-CH_2-(O-C**H$_2$**-C**H$_2$**)$_n$-, m, 58H), 3.22 (C**H$_3$**O-CH_2-CH_2-(O-CH_2-CH_2)$_n$-, s, 3H), 2.54 (-(O-CH_2-CH_2)$_n$-O-CH_2-CH_2-O-C=O-C**H$_2$**-C**H$_2$**-C=O-OH, s, 4H); FT-IR(cm^{-1}) CH-stretching at 2867.53, C=O stretching at 1735.06 and C-O stretching at 1100.47; MALDI-TOF(m/z) MW. range 700-1100.

2.4 Synthesis of the mPEO-CUR-PA

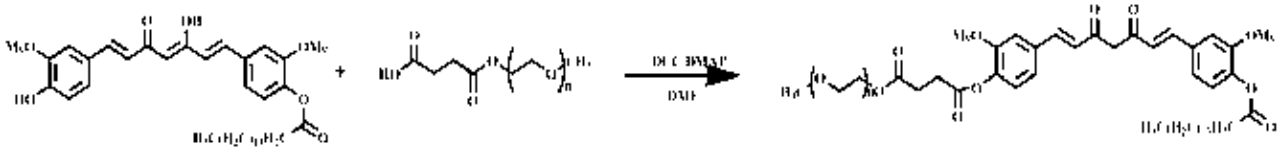

Scheme 2.3 Synthesis of the mPEO-CUR-PA.

The attachment of mPEO-COOH with CUR-PA was carried out through esterification reaction using dicyclohexylcarbodiimide (DCC) and 4-(N,N-dimethylamino)pyridine (DMAP) as coupling agents. DCC (48 mg, 0.2 mmol) was added to the solution of mPEO-COOH (0.1 g, 0.1 mmol) in dry CH_2Cl_2 (5.0 ml). The

mixture was stirred at 0 °C under nitrogen atmosphere for 15 min. Then catalytic amount of DMAP was added to the mixture and stirred at 0 °C for 60 min. The solution of CUR-PA (0.14 g, 0.2 mmol) in dry CH_2Cl_2 (10.0 ml) was added to the mixture, and stirring was continued at room temperature overnight (Scheme 2.3). Crude product was purified on Sephadex column, using 100% MeOH. DCC in the eluted product was eliminated by repeatedly precipitation with cold CH_2Cl_2. Then unreacted CUR-PA and CUR were partially removed by precipitation in methanol. Then the product was subjected to Sephadex column chromatography, using 100% MeOH. Then the liquid product was dispersed in water and further purified by centrifugation with filtering centrifuge (Millipore MWCO 100,000) to obtain 43.78% of mPEO-CUR-PA. The product was characterized by ^{1}H-NMR, FT-IR, UV-visible absorption and MALDI-TOF spectroscopy.

mPEO-palmitoylcurcumin (mPEO-CUR-PA): ^{1}H-NMR ($CDCl_3$, 400 MHz,δ, ppm) 7.46 – 7.67 (Ar-C**H**=CH-C=O-CH_2-C=O-CH=C**H**-Ar-, m, 2H), 6.98-7.14 (m, 6H), 6.53 (Ar-CH=C**H**-C=O-CH_2-C=O-C**H**=CH-Ar-, d, J = 15.9 Hz, 2H), 5.83 (-C=O-C**H$_2$**-C=O-, s, 2H), 4.21 – 4.27 (-(O-CH_2-CH_2)$_n$-O-C**H$_2$**-C**H$_2$**-O-C=O- m, 4H), 3.83 (s, 6H), 3.49 – 3.70(-CH_2-CH_2-(O-C**H$_2$**-C**H$_2$**)$_n$-O, m, 58H), 3.34 (C**H$_3$**O-CH_2-CH_2-(O-CH_2-CH_2)$_n$-, s, 3H), 2.89 (-(O-CH_2-CH_2)$_n$-O-CH_2-CH_2-O-C=O-CH_2-C**H$_2$**-C=O-O-Ar, dd, J = 14.3, 7.5 Hz, 2H), 2.75 (-Ar-O-C=O-C**H$_2$**-CH_2-(CH_2)$_n$-, t, J = 6.8 Hz, 2H), 2.54 (-(O-CH_2-CH_2)$_n$-O-CH_2-CH_2-O-C=O-C**H$_2$**-CH_2-C=O-O-Ar-, dd, J = 15.1, 7.6 Hz, 2H), 1.65 – 1.80 (-Ar-O-C=O-CH_2-C**H$_2$**-(CH_2)$_n$-, m, 2H), 1.05 – 1.49 (-Ar-O-C=O-CH_2-CH_2-(C**H$_2$**)$_n$-, m, 24H), 0.84 (-Ar-O-C=O-CH_2-CH_2-(CH_2)$_n$-C**H$_3$**, t, J = 6.6 Hz, 3H) ; UV-visible spectroscopy(MeOH) λ_{max} at 400 nm, FT-IR(cm^{-1}) CH-stretching at 2917.34 and 2857.56, C=O stretching at 1764.94, C-O stretching 1735.06 and CH-bending at 1116.23 and 1021.99; MALDI-TOF(m/z) MW. range 1000-1500.

2.5 Critical micelle concentration

The pure liquid mPEO-CUR-PA was put in deionization water and sonicated for 30 min to get liquid mixtures at various concentrations (2.0, 8.0, 16.0, 20.0, 40.0, 60.0, 80 and 100 μM). The critical micelle concentration (CMC) of mPEO-CUR-PA was determined by measuring an ability to scatter light of these mixtures. Light scattering was acquired in a 1 cm path-length quartz cuvette with the use of monochromatic laser radiation set perpendicularly to the detector (533 nm, at 100mW) as light source and the ocean optics® USB2000 as detector.

2.6 Encapsulation of paclitaxel

Paclitaxel solution in DMSO was added to the water suspension of mPEO-CUR-PA and sonicated for 30 min to obtain paclitaxel loaded mPEO-CUR-PA micelles. The amount of DMSO in the final suspension was less than 1 % (v/v). The encapsulation was prepared at the paclitaxel to mPEO-CUR-PA mole ratios of 0.001: 100, 0.01:100, 0.1:100 and 1.0:100.

2.7 Paticle characterization

Shape and size of unloaded and paclitaxel loaded mPEO-CUR-PA micelles were characterized by confocal microscopy using both differential interference contrast (DIC) mode and fluorescent mode. In the fluorescent mode, fluorescent signals (420-750 nm) of the samples were collected at various depths of the samples. The fluorescent spectral components of curcumin in mPEO-CUR-PA micelles was detected and confirmed with the obtained spectrum using chemometric analysis (image algorithms) based on the spectral database constructed from fluorescent spectra of pure curcumin through the Nikon-C1-Si software (Nikon, Tokyo, Japan). Suspensions of particles in water at the 100.0 μM and paclitaxel loaded micelles in various ratios were also subjected to dynamic light scattering (Zetasizer nanoseries

model S4700, Malvern Instruments, Worcestershire, UK) for the hydrodynamic size determination.

2.8 Cellular uptake of mPEO-CUR-PA

The uptake of mPEO-CUR-PA was investigated on HEp-2 human laryngeal carcinoma cells. The HEp-2 cells were grown in RPMI 1640 medium (GIBCO BRL, Life Technologies Inc., NY, USA) supplemented with 2.05 mM L-Glutamine (Hyclone Laboratory, Inc., Logan, UT, USA), 10% (v/v) fetal bovine serum (Hyclone), and 1% (v/v) antibiotic-antimycotic solution (GIBCO), at 37^{o}C in a humidified atmosphere of 5% CO_2.

The HEp-2 cells were seeded into a 6-well plate in 1 ml of culture media and allowed to adhere overnight. The following day, cells were treated with mPEO-CUR-PA, and incubated at 37 °C in a CO_2 incubator for 2 h. Then the media was removed and the cells were washed with RPMI 1640 medium two times. After that, the cells were incubated with 100 mg l^{-1} acridine orange for 1 h, then media was removed, and the cells were washed with RPMI 1640 medium before being subjected to the confocal laser fluorescent microscopic analysis (Nikon Digital Eclipse C1-Si/C1Plus (Tokyo, Japan) equippedwith Plan Apochromat VC 100×, a 32-channel-PMT-spectral-detector, and Nikon-EZ-C1 software. Excitation was carried out using Diode Laser (405 nm, Melles Griot, Carlsbad, CA, USA), and fluorescent spectral signals at 420–750 nm were collected. The obtained spectra of each pixel were then unmixed into mPEO-CUR-PA and acridine orange components, using chemometric analysis (image algorithms) based on the spectral database constructed from fluorescent spectra of standard mPEO-CUR-PA and acridine orange which was stained on the HEp-2 cells, through the EZ-C1 software (Nikon, Tokyo, Japan). Image indicating locations of mPEO-CUR-PA was then constructed using the obtained resolved signals.

2.9 In vitro antitumor assay

Paclitaxel loaded microsphere, unloaded microspheres, unencapsulated paclitaxel (in DMSO) were test with HCC-S102, A549 and A549RT/eto cells.

2.9.1 Cell culture

HCC-S102 human hepatocellular carcinoma cell line was established from a Thai patient [51]. A549 human lung adenocarcinoma cell line was obtained from the American Type Culture Collection (ATCC). A549RT-eto, a multidrug resistant cancer cell line was developed from A549 cells [52]. All cell lines were grown in RPMI 1640 medium supplemented with 10% (v/v) fetal bovine serum, and 1% (v/v) antibiotic-antimycotic solution, at 37^{o}C in a humidified atmosphere of 5% CO_2.

2.9.2 Cell viability assay

Cell viability was determined the MTT method [53] with some modifications. Briefly, cell suspensions inculture medium were seeded in 96-well plates (100 μL/well) and incubated at 37 ^{0}C in a humidified atmosphere of 5% CO_2. After 24 h, additional medium (100 μL) containing test sample was added to each well, followed by further incubation for 24 and 72 h. Then, the wells were replaced and incubated with fresh culture media containing of (3-[4, 5-dimeylthiazol-2-yl]-2, 5-diphenyltetrazolium bromide) (MTT, Sigma-Aldrich Chemical Co., St.Louis, MO, USA) (0.5mg/mL) for 2 h at 37 ^{0}C. Finally, the media were removed and DMSO was added to the wells (100 μL/well), and absorbance was measured at 550 nm in a microplate reader. Normally, the color of MTT dye is yellow with the maximum absorption wavelength of 650 nm. When incubated with the metabolically active cells, MTT will be reduced into insoluble purple formazan dye crystals which absorbs the 550 nm light. The number of viable cells can be determined from the difference in the absorbance at 550 nm and that at 650 nm. Assays were performed in triplicate. Data were expressed as percent viability compared with control.

The cancer cells were incubated with mPEO-CUR-PA microspheres at five final concentrations; 12.8, 32.0, 80.0, 200.0 and 500.0 μM. The final concentrations of drug-loaded microsphere are showed in Table2.1.

Table 2.1 Final concentrations of paclitaxel:mPEO-CUR-PA in the cytotoxicity tests

HCC-S102 paclitaxel:mPEO-CUR:PA (μM)	**A549 paclitaxel:mPEO-CUR-PA (μM)**	**A549-eto paclitaxel:mPEO-CUR-PA (μM)**
0.01:100	0.1:100	0.1:100
0.001:100	0.01:100	0.01:100
0.0001:100	0.001:100	0.001:100
0.00001:100	0.0001:100	0.0001:100

CHAPTER III

RESULTS AND DISCUSSION

3.1 Synthesis and characterizations

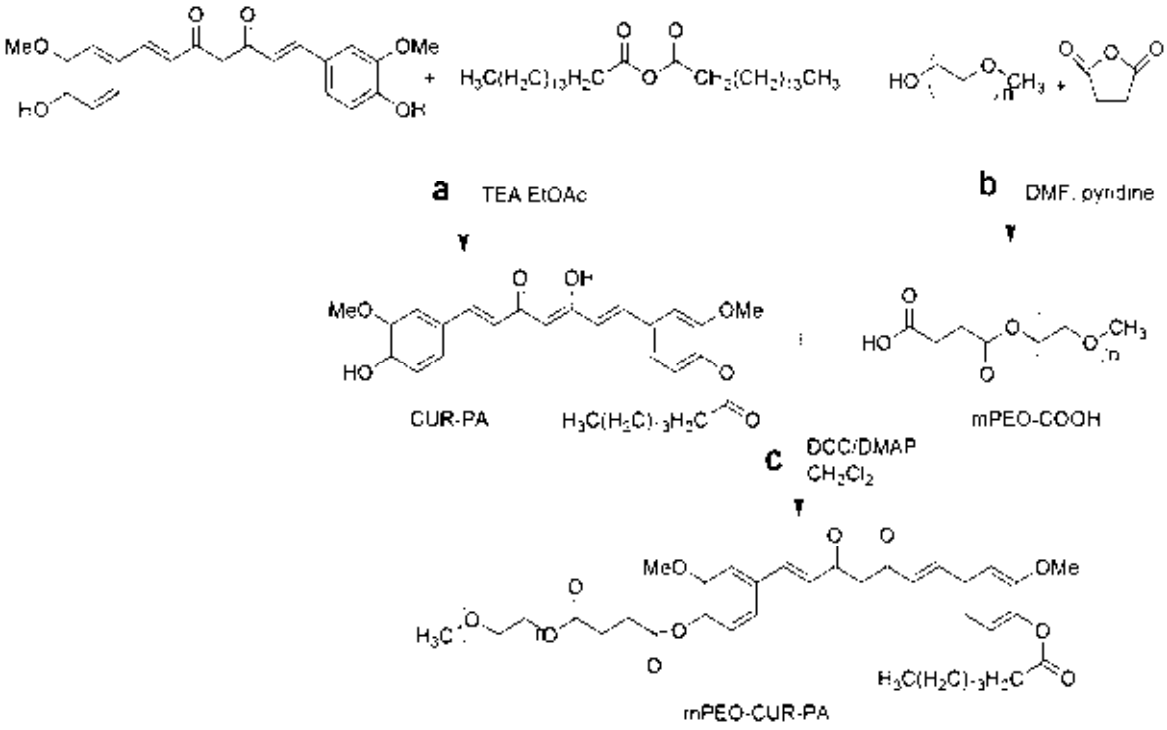

Scheme 3.1 (a) Synthesis of palmitoylcurcumin (CUR-PA). (b) Synthesis of methoxy poly(ethylene oxide) acetic acid (mPEO-COOH). (c) Synthesis of the mPEO-CUR-PA.

3.1.1 Synthesis of palmitoylcurcumin (CUR-PA)

The synthesis pathway of palmitoylcurcumin (CUR-PA) is shown in Scheme 3.1(a). Palmitoylcurcumin was synthesized by reaction between hydroxyl groups of curcumin and carbonyl groups of palmitic anhydride. Hydroxyl groups of curcumin

were deprotonated by triethylamine and carbonyl groups of palmitic anhydride reacted as nucleophile to form ester bond. The mechanism is shown in Scheme 3.2

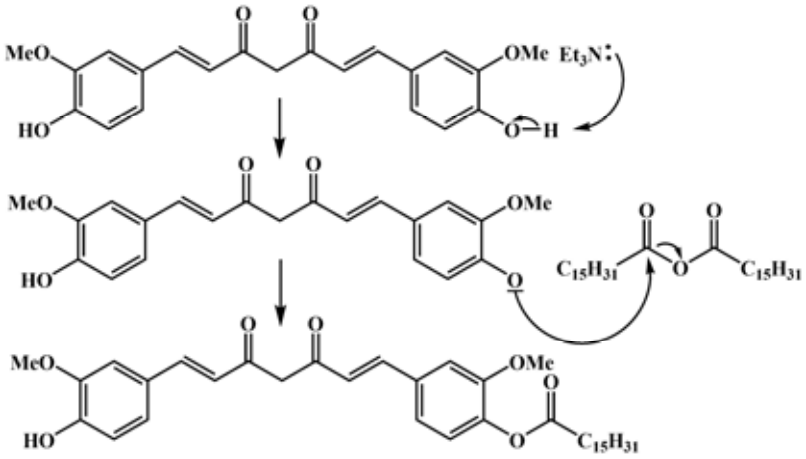

Scheme 3.2 Mechanism of synthesis of palmitoylcurcumin(CUR-PA).

In this step, temperature and ratios of reactants are critical factors that control the amount of mono-substitution product. The temperature of 0^{o} C was used in order to slow down the rate of reaction. Various mole ratios of curcumin:palmitic anhydride were experimented (Table 3.1).

Table3.1 The mole ratios of curcumin:palmitic anhydride

Molar ratio Curcumin:Palmitic anhydride	**% yield of mono-substitution product**
1.0:1.0	19.22
3.0:1.0	35.57
5.0:1.0	52.28
7.0:1.0	38.23

According to the Table 3.1, mole ratios of curcumin:palmitic anhydride at 5:1 gave 52.28 % yields of the mono-substituted palmitoylcurcumin. As a result, this molar ratio was selected as the optimal condition for the preparation of CUR-PA. The crude form reaction was purified by silica gel column chromatography using 20-40% EtOAc gradient in hexane and reprecipitate in MeOH to obtain the pure palmitoylcurcumin as yellow powder.

The product was confirmed by ^{1}H-NMR (Figure3.1 (b)); signals of curcumin at 6.93-7.17 ppm (Ar-**H**), 7.60 ppm (Ar-C**H**=) and 6.46-6.58 ppm (=C**H**C(O)-), 5.83-5.88 ppm (-C(O)C**H**C(O)-), and signals of palmitate moiety at 0.88-1.46 ppm.

When comparing the ^{1}H-NMR spectrum of palmitoylcurcumin to that of the curcumin, it is obvious that the signals of methoxy proton ($H_{p,q}$) of CUR-PA are splitted into two-singlet peaks at ratio of H_p:H_q of 1:1 (comparing to one singlet peak for the unmodified curcumin). This agrees with the fact that the molecule of palmitolycurcumin is not symmetry while the curcumin molecule is symmetry, thus the two methoxy groups of curcumin are equivalent. The molecular weight of CUR-PA were determined by MALDI-TOF technique found the molecular ion at 607.7 (m/z), agreeing with the calculated M.W. (607.0) (Figure 3.2).

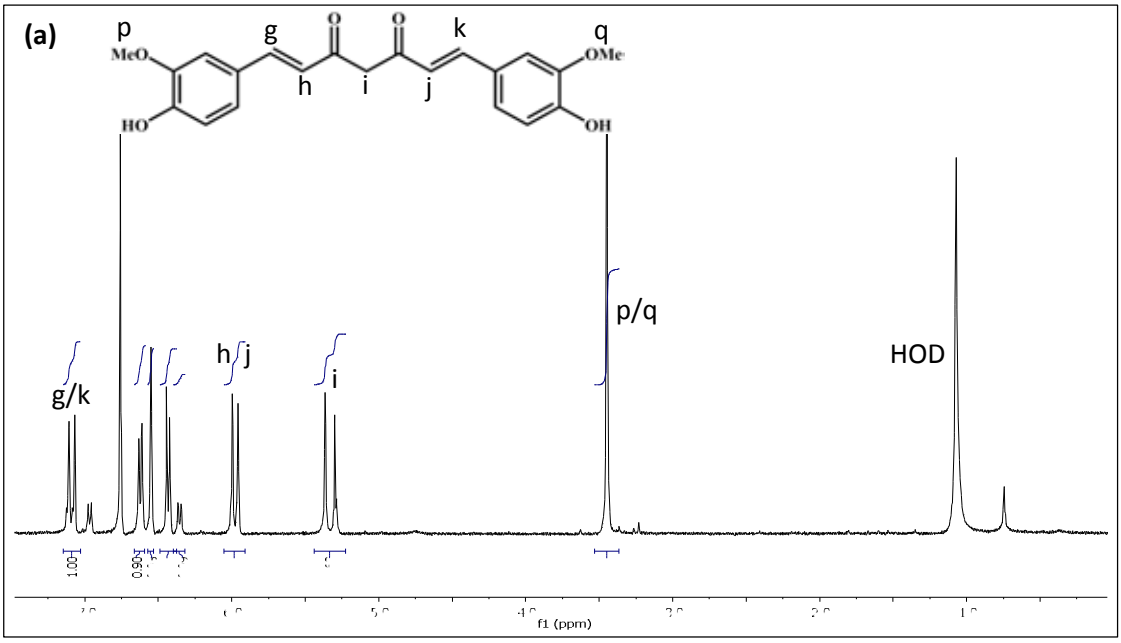

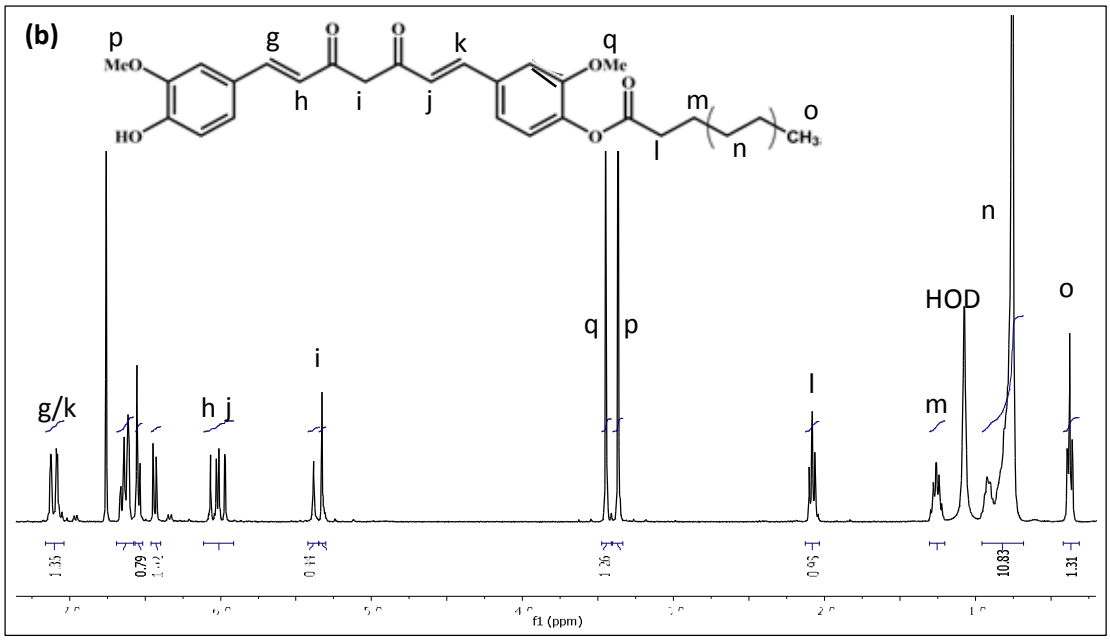

Figure 3.1 [1]H-NMR spectrum of (a)Curcumin and (b)palmitolycurcumin(CUR-PA)

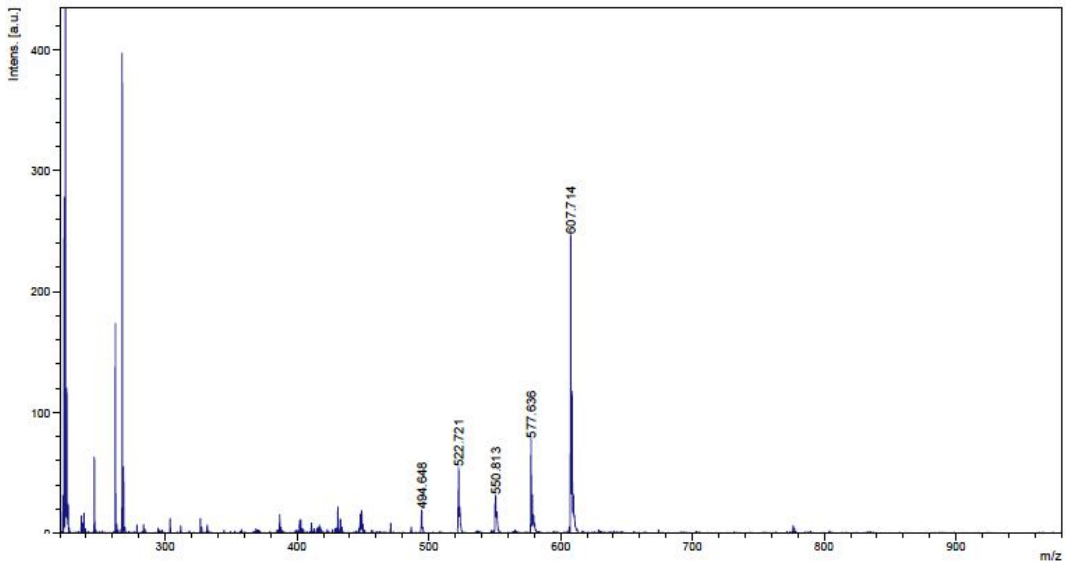

Figure3.2 Mass spectrum (MALDI-TOF) of CUR-PA

3.1.2 Synthesis of methoxy poly(ethylene oxide) acetic acid (mPEO-COOH)

The synthesis pathway of mPEO-COOH is shown in Scheme 3.1(b). The hydroxyl group of the methoxy polyethylene glycol polymer (mPEO) was acylated by treatment with succinic anhydride. Mechanistically, hydroxyl group of mPEO was deprotonated by pyridine to obtain the hydroxyl anion as nucleophile. The ring-opening reaction occurred upon the nucleophile attack with succinic anhydride. The mechanism is shown in Scheme 3.3

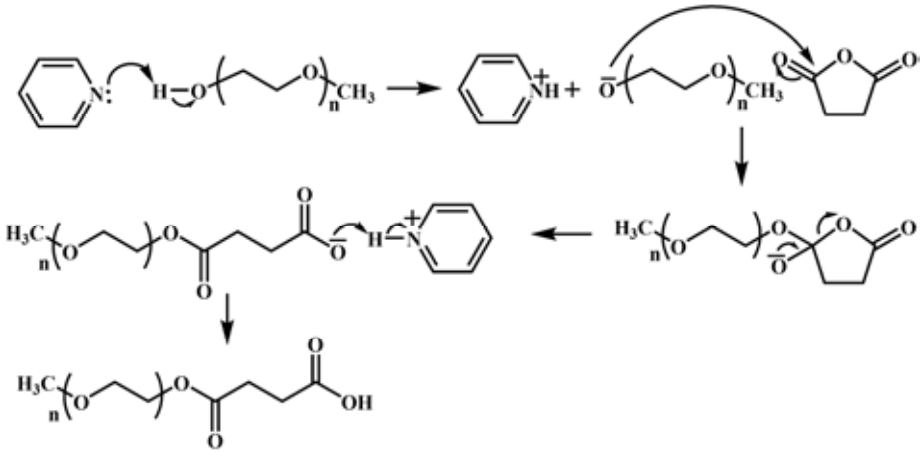

Scheme 3.3 Mechanism of synthesis of methoxy poly(ethylene oxide) acetic acid (mPEO-COOH)

The obtained mPEO-COOH was purified through Sephadex column to eliminate the excess succinic acid and partially eliminate mPEO.

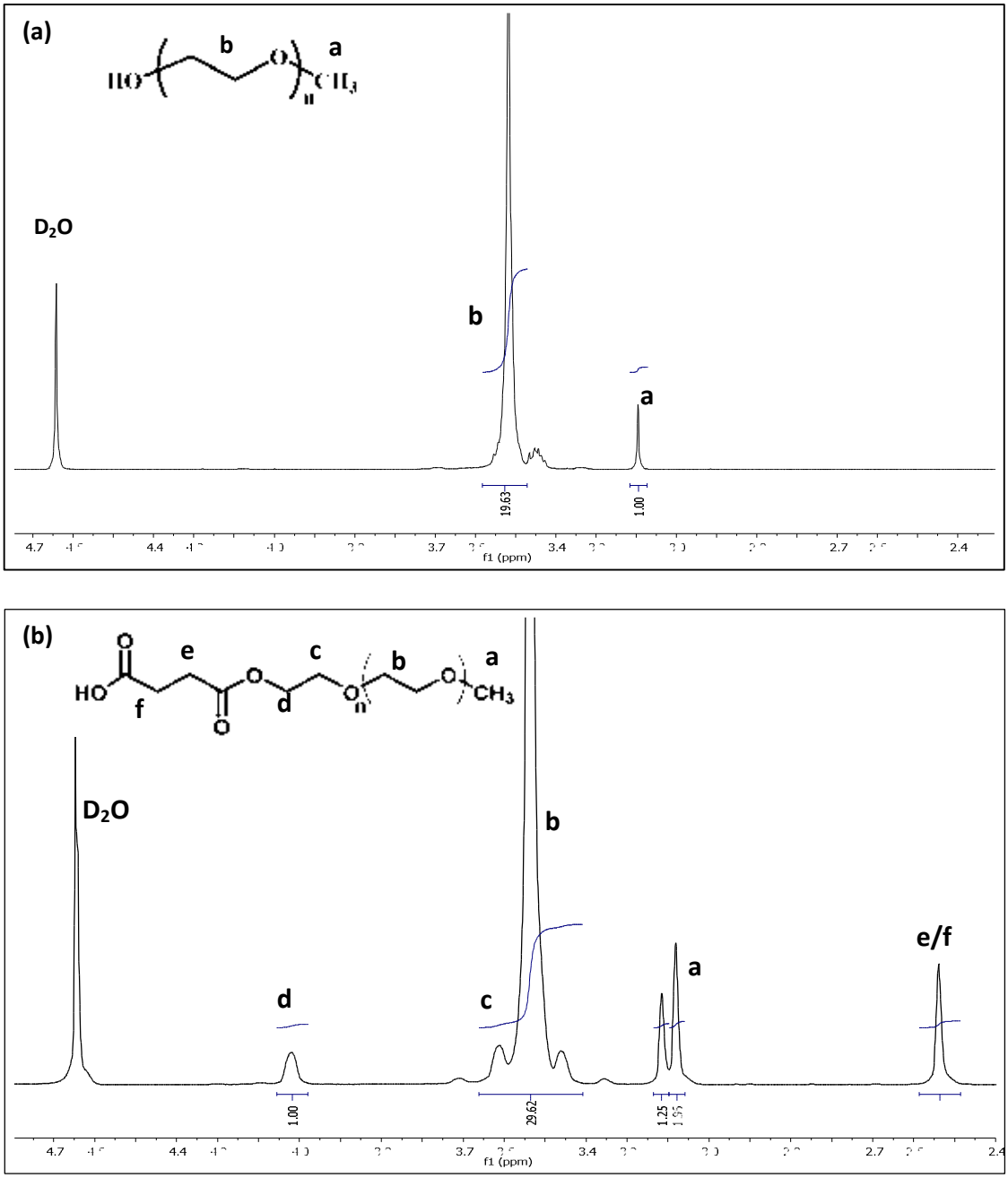

Figure 3.3 ^{1}H-NMR spectrum of (a) methoxy poly(ethylene glycol)(mPEO) and (b) methoxy poly(ethylene glycol) acetic acid (mPEO-COOH)

^{1}H-NMR spectrum of mPEO-COOH product (Figure 3.3) shows signals of ethylene oxide protons (-O-C**H**$_2$C**H**$_2$-O-) at 3.41-3.66 ppm and acetic protons (-C(O)-C**H**$_2$-C**H**$_2$-C(O)-) at 2.54 ppm. Signals from terminated methoxy protons of both

mPEO-COOH and mPEO at 3.22 and 3.18 ppm, respectivelycould be observed, indicating the presence of mPEO species in the mPEO-COOH product. Estimated from the proton NMR integration, the amount of mPEO-COOH in the mixtures was 40.32%. This results in the calculated yield of 9.39 % by mol. The molecular weight range of mPEO-COOH was 700-1100 (m/z) as determined by MALDI-TOF (Figure 3.4).

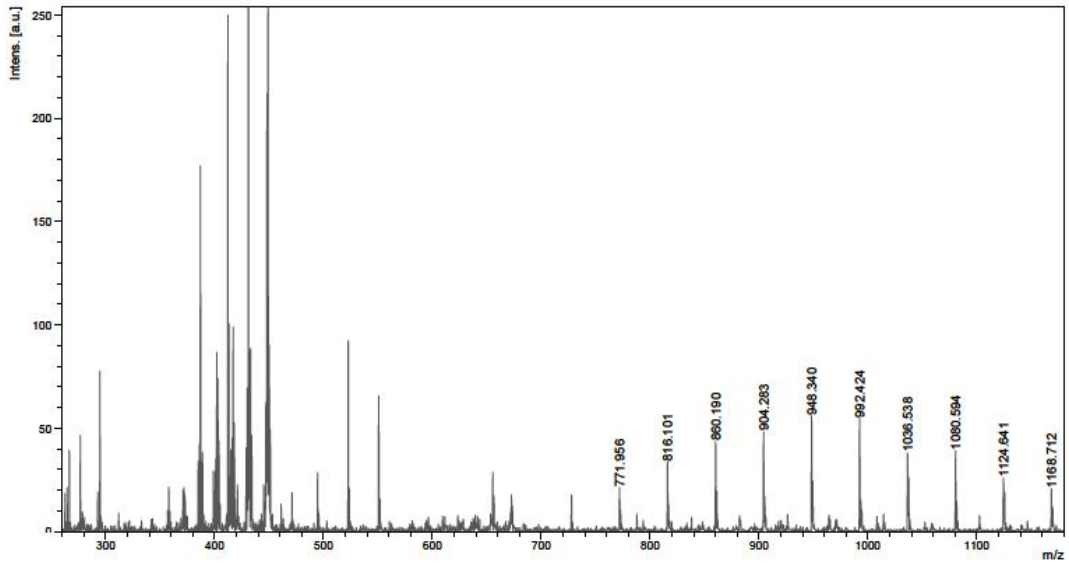

Figure 3.4 Mass spectrum (MALDI-TOF) of mPEO-COOH

3.1.3 Synthesis of the mPEO-CUR-PA conjugate

mPEO-CUR-PA was synthesized by Steglich esterification using dicyclohexylcarbodiimide (DCC) as a coupling reagent and 4-dimethylaminopyridine (DMAP) as a catalyst. This reaction generally takes place at room temperature and the suitable solvent is dichloromethane. The carboxylic group of mPEO-COOH was reacted with DCC to form an O-acyl isourea, which is more reactive than the free acid. After that DMAP, a stronger nucleophile comparing to alcohol, reacts with O-acyl isourea leading to the formation of a reactive amide intermediate. This intermediate cannot form intramolecular side product but reacts rapidly with hydroxyl group of the CUR-PA, forming ester bond, and the mPEO-CUR-PA is produced. Therefore, DMAP acts as an acyl transfer reagent. In this reaction DCC was hydrated

by water to form urea by product, dicyclohexylurea (DHU). The mechanism is shown in Scheme 3.4.

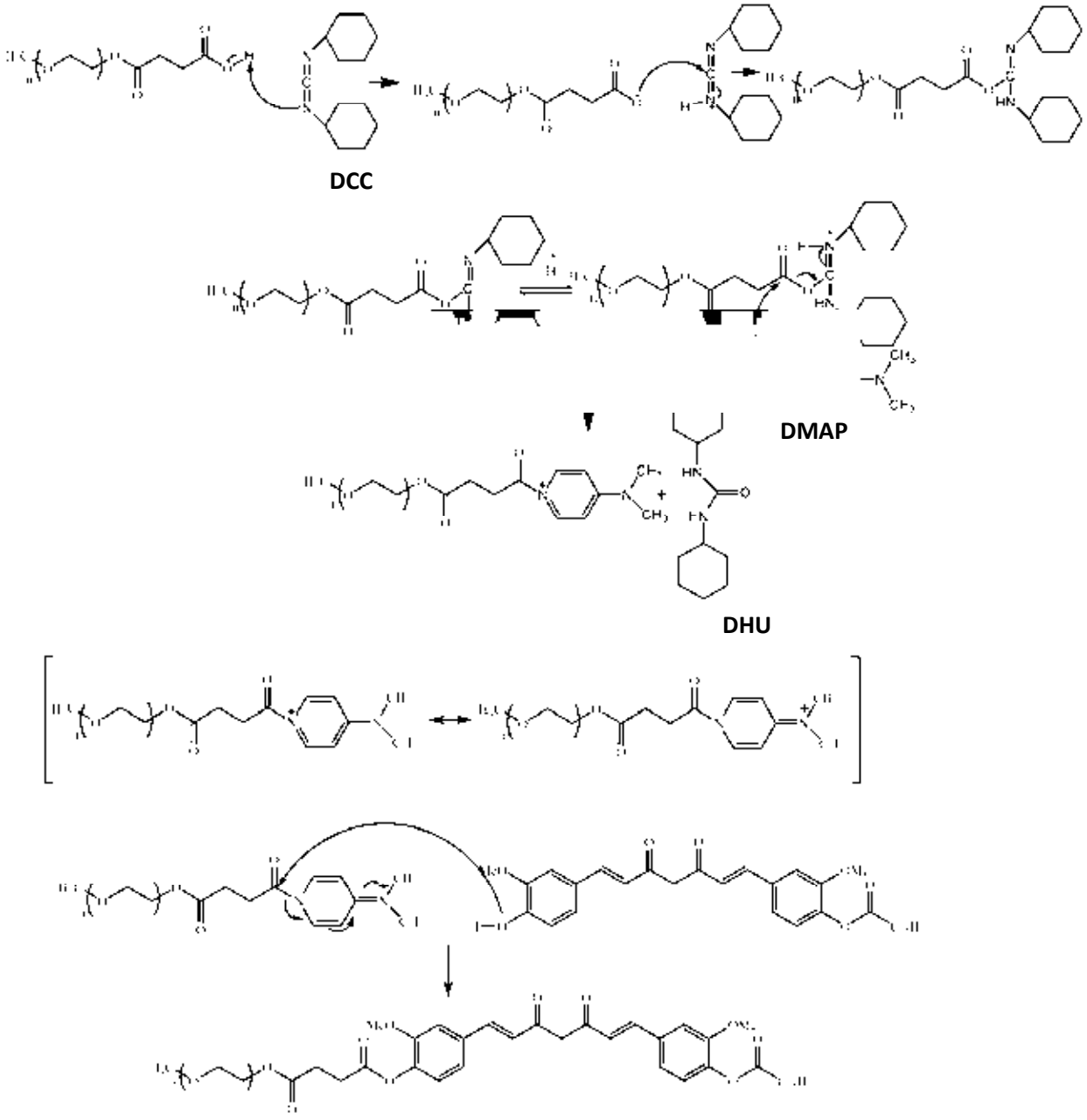

Scheme 3.4 Mechanism of synthesis of mPEO-CUR-PA conjugate

The obtained mPEO-CUR-PA was purified through Sephadex column, multiple DCC precipitations in cold CH_2Cl_2, followed with filtering centrifugation using the membrane of M.W. cut-off of 100,000 which could retain the self-assembled mPEO-CUR-PA microspheres while letting the left-over mPEO-COOH pass through.

The product was confirmed by ^{1}H-NMR spectrum (Figure3.5); signals of mPEO at 3.49-3.70 ppm, curcumin at 6.98-7.67 ppm and palmitate moiety at 0.84-1.49 ppm.

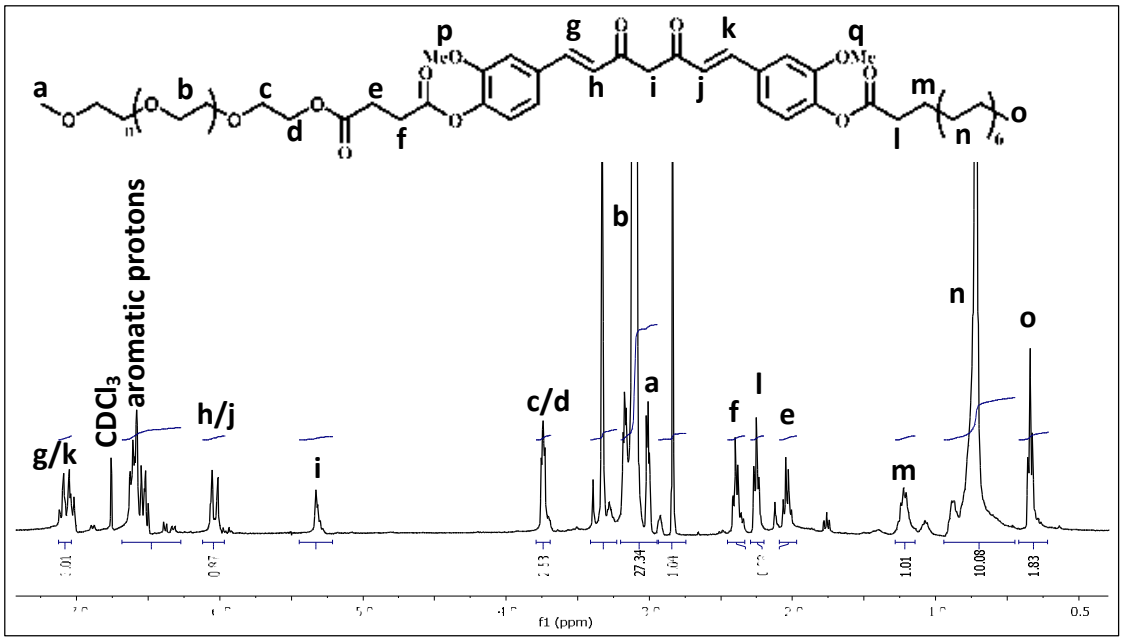

Figure 3.5 ^{1}H-NMR spectrum of mPEO-CUR-PA conjugate

^{1}H-NMR spectrum of mPEO-CUR-PA (Figure 3.5) showed the ratios of mPEO proton:palmitate proton of 2.7:1.0 which is close to the calculated ratios of 2.4:1.0, therefore, confirming that we have obtained reasonably pure mPEO-CUR-PA product. The molecular weight range of mPEO-CUR-PA is 1000-1500(m/z) as determined by MALDI-TOF (Figure 3.6).

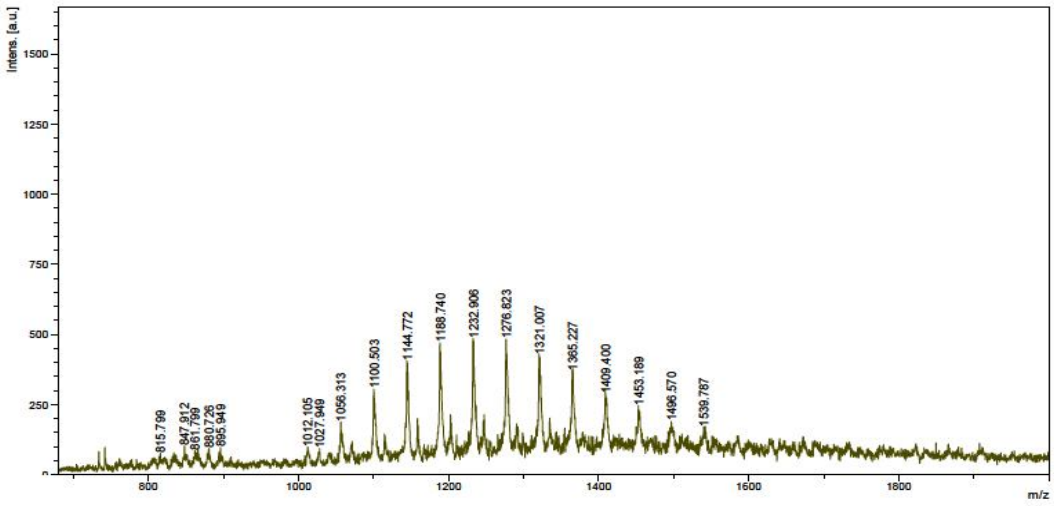

Figure3.6 Mass spectrum (MALDI-TOF) of mPEO-CUR-PA

3.1.4 UV-visible spectroscopy

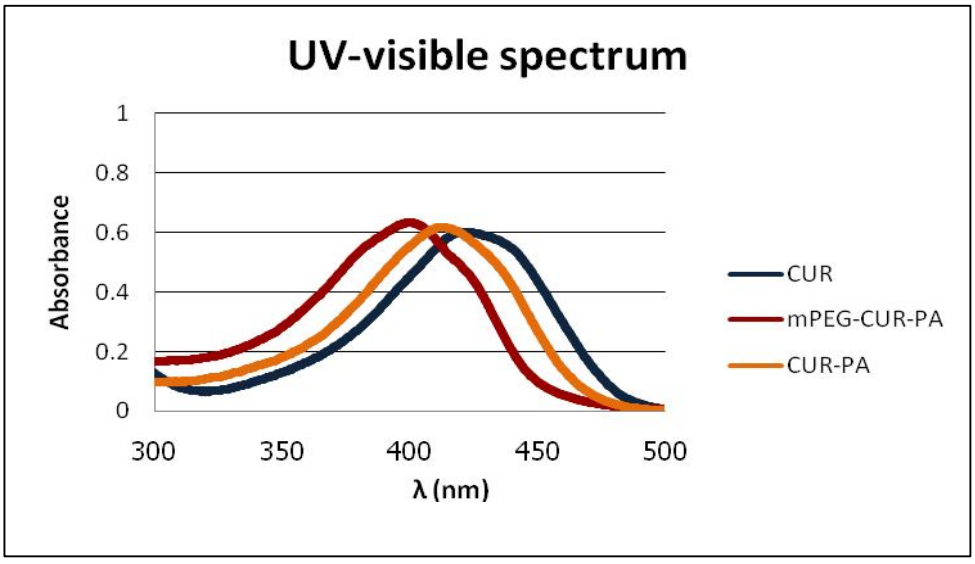

Figure 3.7 UV-visible absorption spectrum of CUR, CUR-PA and mPEO-CUR-PA

The solution of curcumin and curcumin derivatives in methanol showed a board characteristic UV-vis absorption around 320-480 nm. From the Figure 3.7, UV-visible absorption spectrum showed λ_{max} of curcumin, palmitoylcurcumin and mPEO-CUR-PA conjugate at 428, 418 and 409 nm respectively. Maximum wavelength of CUR-PA and mPEO-CUR-PA is blue-shifted from that of free curcumin. The blue-shift indicated less conjugation in the curcumin core structure resulting from the replacement of hydroxyl group (electron donating group) to the acyl group (electron-withdrawing group).

3.1.5 ATR-FT-IR spectroscopy

The obtained product was analyzed using ATR-FT-IR. The first, FT-IR spectrum of mPEO-COOH (Figure 3.8 (a)) showed the absorption peaks at 1735.06 cm^{-1} corresponded to C=O stretching vibration, indicating the new ester functionality, and the absorption peaks at 1100.74 cm^{-1} corresponded to C-O stretching vibration, indicating the ethylene oxide groups of mPEO. Second, FT-IR spectrum of CUR-PA (Figure 3.8 (b)) showed the absorption peaks at 2847.60 and 2914.02 cm^{-1} corresponded to C-H stretching vibration, indicating the palmitate moiety. Moreover, the peaks around 1754.98 and 1625.46 cm^{-1} could be assigned to C=O stretching frequency of keto-enol functionality of curcumin. The third, FT-IR spectrum of mPEO-CUR-PA (Figure 3.8(c)) showed the absorption peaks of mPEO around 1116.23 and 1021.99 cm^{-1}, the C-H stretching peak of palmitate at 2917.34 and 2857.56 cm^{-1}, and the C=O stretching of curcumin at 1764 and 1735 cm^{-1}.

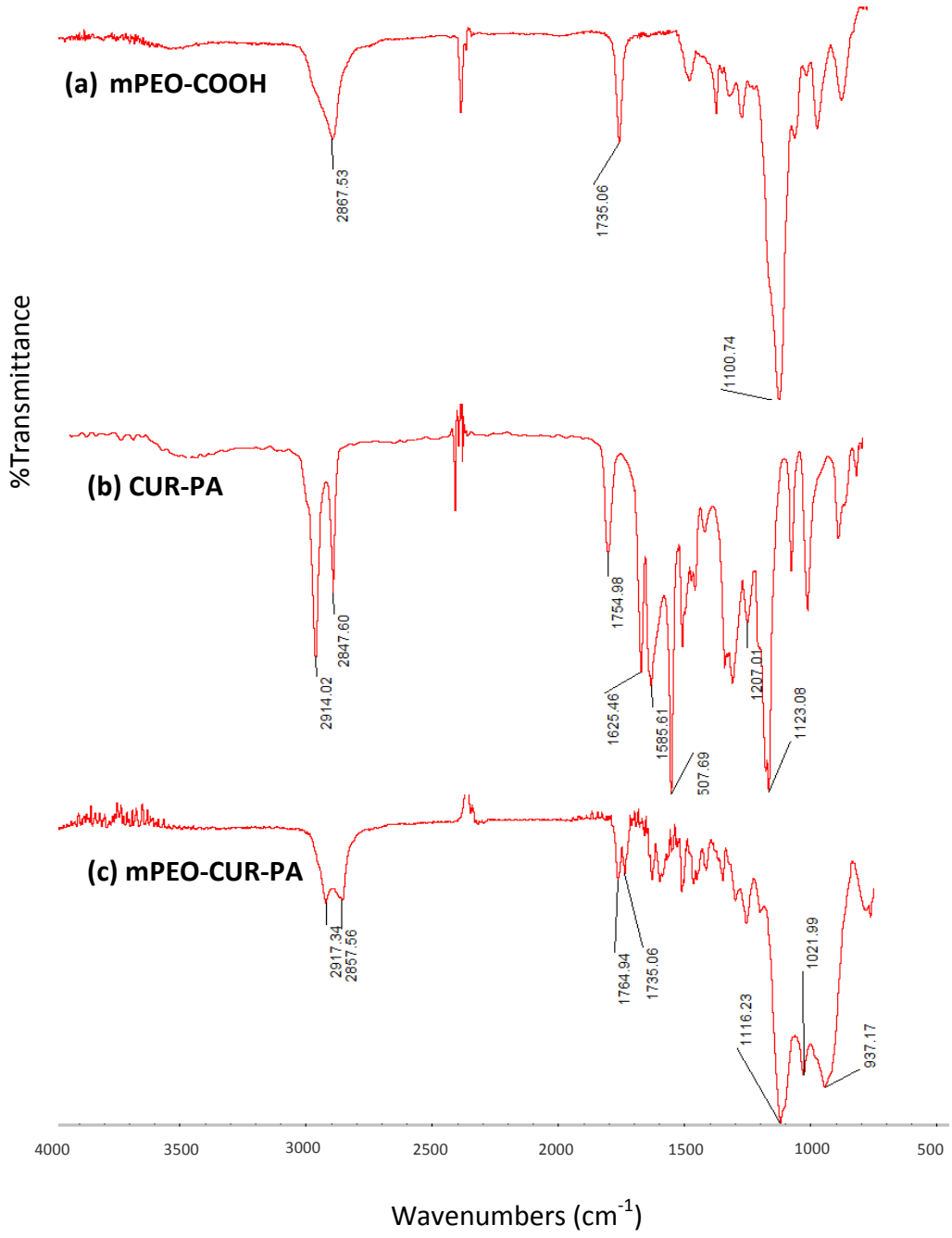

Figure 3.8 FT-IR spectra of (a)mPEO-COOH, (b)CUR-PA and (c)mPEO-CUR-PA

From the above spectroscopic characterization, the chemical structure of mPEO-CUR-PA,an intense yellowish liquid, could be clarified.

3.2 Self-assemble of mPEO-CUR-PA

The mPEO-CUR-PA structure (Figure 3.9) is designed as an amphiphillic molecule in which the PA is the hydrophobic segment and the mPEO is the hydrophilic segment. The PEO was chosen not only because of its hydrophillicity, but also because PEO is non-toxic, biocompatible, and possesses stealth characteristic with the immune system.

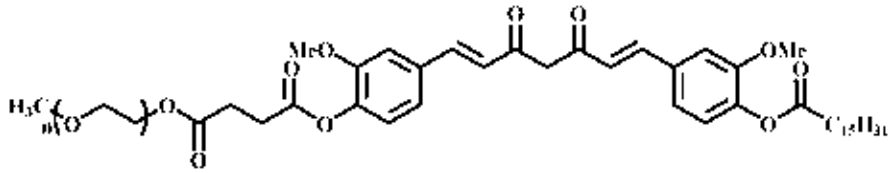

Figure 3.9 Structure of mPEO-CUR-PA

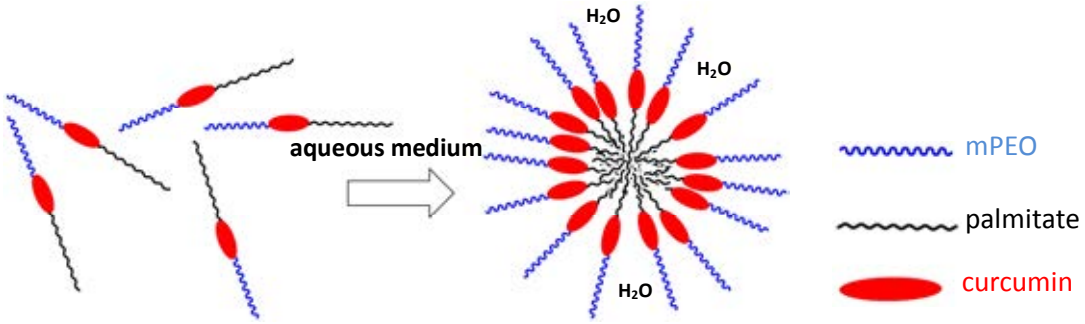

Figure 3.10 The self-assembling of mPEO-CUR-PA micelles in aqueous medium

During self-assembling in water (Figure 3.10), the PA moieties should arrange themselves to be at the core of the micelles in order to have minimum contact with water molecules, while the PEO moieties should be directed outward to have maximum interaction with aqueous medium. The presence of PA should increase the hydrophobic interaction at the micellar core thus making the spheres more stable, while the presence of the mPEO at the outer surface should make the sphere water dispersible.

3.3 Critical micelles concentration(CMC)

The self-assembly behavior of amphiphillic polymer in aqueous solution was characterized by measuring the critical micelles concentration (CMC) of mPEO-CUR-

PA conjugate using light scattering technique, the scattering intensity of mPEO-CUR-PA at various concentrations are shown in Figure 3.11. At low concentrations, the number of amphiphillic polymeric chains was not enough to form micelles and therefore they were soluble in water (minimal light scattering). At concentration above 20 μM, the amphiphillic polymers started to form micelles. The presence of micelles causes the solution to be more turbid, thus increasing of light scattering could be observed at 40-100 μM. In summary, the CMC in water of this amphiphillic molecule is 20 μM.

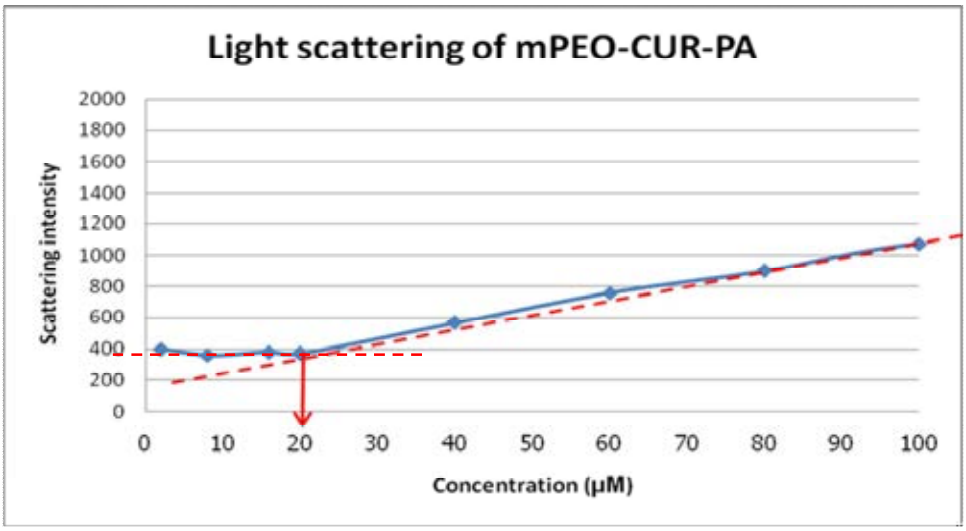

Figure 3.11 Critical micelles concentration of mPEO-CUR-PA in water

3.4 Encapsulation of paclitaxel

Paclitaxel was loaded into the mPEO-CUR-PA spheres by allowing the mPEO-CUR-PA to self-assemble in the presence of paclitaxel under ultrasonic condition. The hydrophobic nature of paclitaxel drove the molecules to move into the hydrophobic core of the spheres (Figure 3.12). After ultrasonication, no paclitaxel crystal could be observed under microscope, indicating well encapsulation of the drug into the mPEO-CUR-PA spheres.

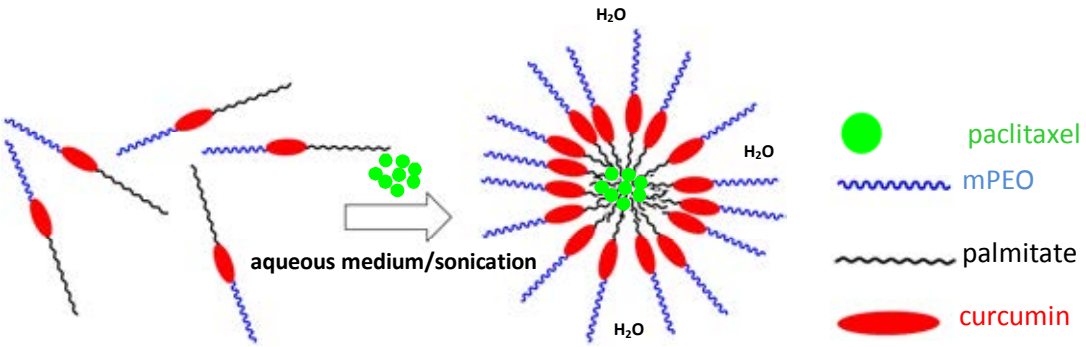

Figure 3.12 Encapsulation of paclitaxel in mPEO-CUR-PA micelles

3.5 Morphology and Hydrodynamic diameter of the micelles

3.5.1 mPEO-CUR-PA micelles

As expected, the mPEO-CUR-PA self-assembled in water into spherical architecture of the size of ~ 1.7 µm as observed by the confocal microscope using the differential interference contrast (DIC) mode (Figure 3.13 (a)). Clear fluorescent signal of the curcumin chromophore from the particles could also be clearly observed through the fluorescent mode of the microscope (Figure 3.13 (f)), thus confirming that the observed spheres were the mPEO-CUR-PA material. Dynamic light scattering also revealed an average hydrodynamic diameter of 1.794 ± 0.197 µm (Table 3.2).

3.5.2 mPEO-CUR-PA micelles with paclitaxel loaded

Microscopic picture in the DIC mode of the obtained mixture clearly showed suspended microspherical architectures with a diameter of approximately ~ 1.5 – 2.0 µm (Figure 3.13(b-e)). The observed size agreed well with the hydrodynamic diameter obtained from the dynamic light scattering experiment were showed in Table3.2

Table 3.2 Hydrodynamic diameter from the dynamic light scattering

Mol ratio of paclitaxel:mPEO-CUR-PA	Hydrodynamic size(μm)
free mPEO-CUR-PA 100 μM	1.794 ± 0.197
0.001:100	2.090 ± 0.299
0.01:100	2.621 ± 0.112
0.1:100	2.556 ± 0.217
1.0:100	2.595 ± 0.267

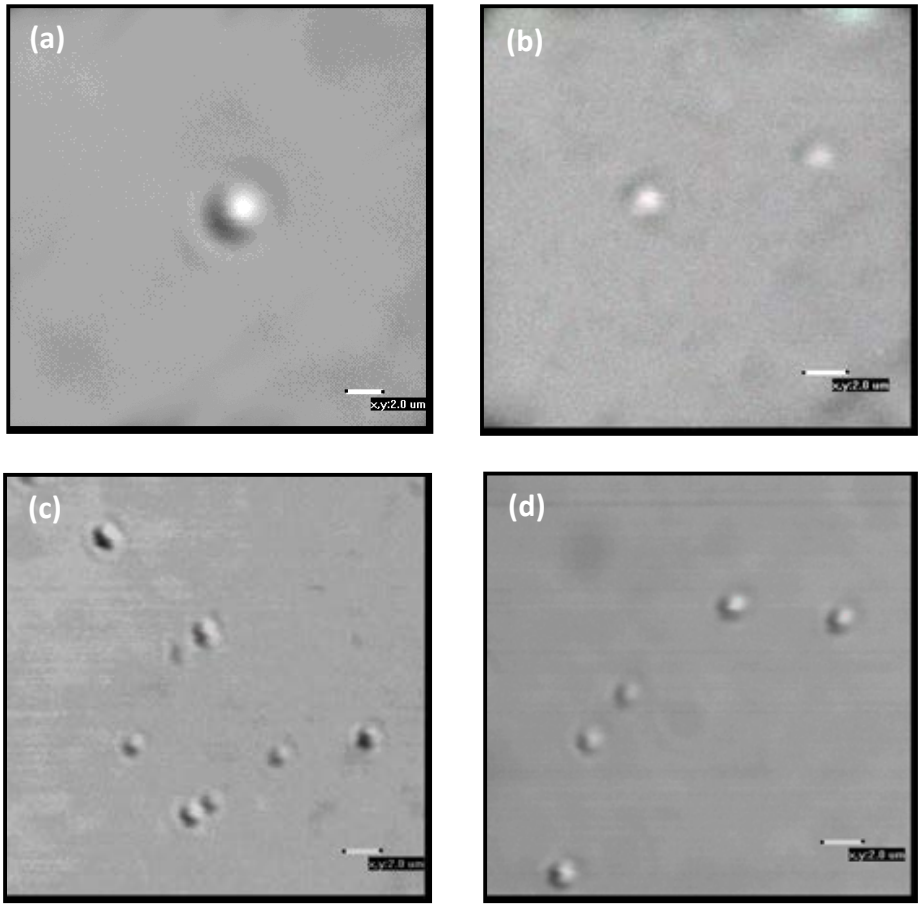

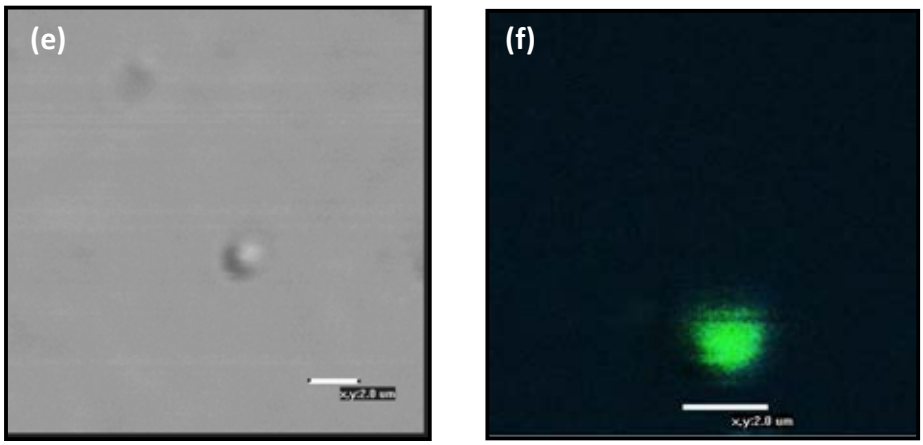

Figure 3.13. Microscopic picture of suspension of **(a)**mPEO-CUR-PA, paclitaxel loaded mPEO-CUR-PA prepared at paclitaxel:curcumin mol ratio; **(b)**0.001:100, **(c)**0.01:100, **(d)** 0.1:100, **(e)**1.0:100 and **(f)** fluorescence picture of curcumin moiety of mPEO-CUR-PA

The hydrodynamic size of the paclitaxel-loaded spheres was a little bigger than the unloaded spheres and the size of the spheres increased with the drug loading.

3.6 Cytotoxicity test with cancer cells

3.6.1 Cytotoxicity test of mPEO-CUR-PA microspheres

The mPEO-CUR-PA microspheres were tested on the S102 and A549 cells. The anti-tumor of mPEO-CUR-PA varied with incubation time at 24 h and 72 h. At 24 h the pro-drug micelles leaded to the increasing of %viability comparing to curcumin (Figure3.14 (a-b)). However, at the 72 h the pro-drug micelles leaded to the decreasing of %viability comparing to the standard curcumin (3.14 (c-d)). The difference here might involve the time required for the availability of active curcumin, releasing from the self-assembled mPEO-CUR-PA which were delivered into cells via endocytosis (see discussion in section 3.6.2 page 48). From this result, we decided to study anti-tumor activity of the pro-drug micelles at 72 h. S102 showed higher anti-tumor activity than the standard curcumin at high concentrations (Figure 3.14(c)). In fact, the activity of mPEO-CUR-PA started to

significantly increase at between 30 - 80 μM, a concentration that is slightly higher than the CMC value (~ 20 μM), and was more effective than the free curcumin at concentrations above 100 μM. We speculate that the increase of cytotoxic activity at the concentration above the CMC value is due to a better cellular uptake of the mPEO-CUR-PA in the self-assembled microspherical form than in the free molecules. Therefore, at high concentration of mPEO-CUR-PA, more drugs could be delivered into cells, thus high anti-tumor activity was observed. In contrast, in the case of unmodified curcumin, high concentration did not make possible the delivery of more drug molecules into cells since the drug itself has limited water solubility.

To make sure that this is not just a co-incidence, experiment with A549 cells was carried out. Similar to the S102 cell line, the anti-tumor activity was obvious at 72 h comparing to the result at 24 h (Figure 3.14(d)). The mortality of A549 also started to increase at the mPEO-CUR-PA concentration above 20 μM (Figure 3.11). This agrees with our speculation of a better uptaking of the material in the form of self-assembled architecture.

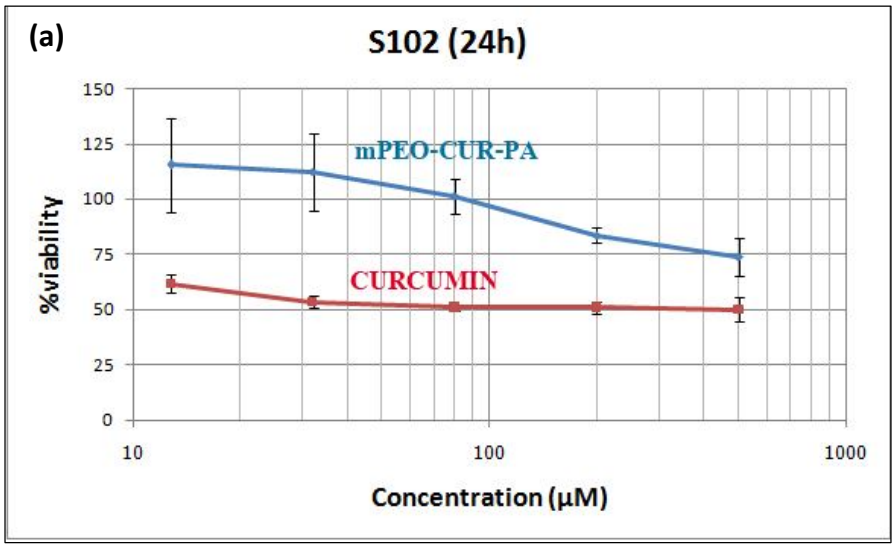

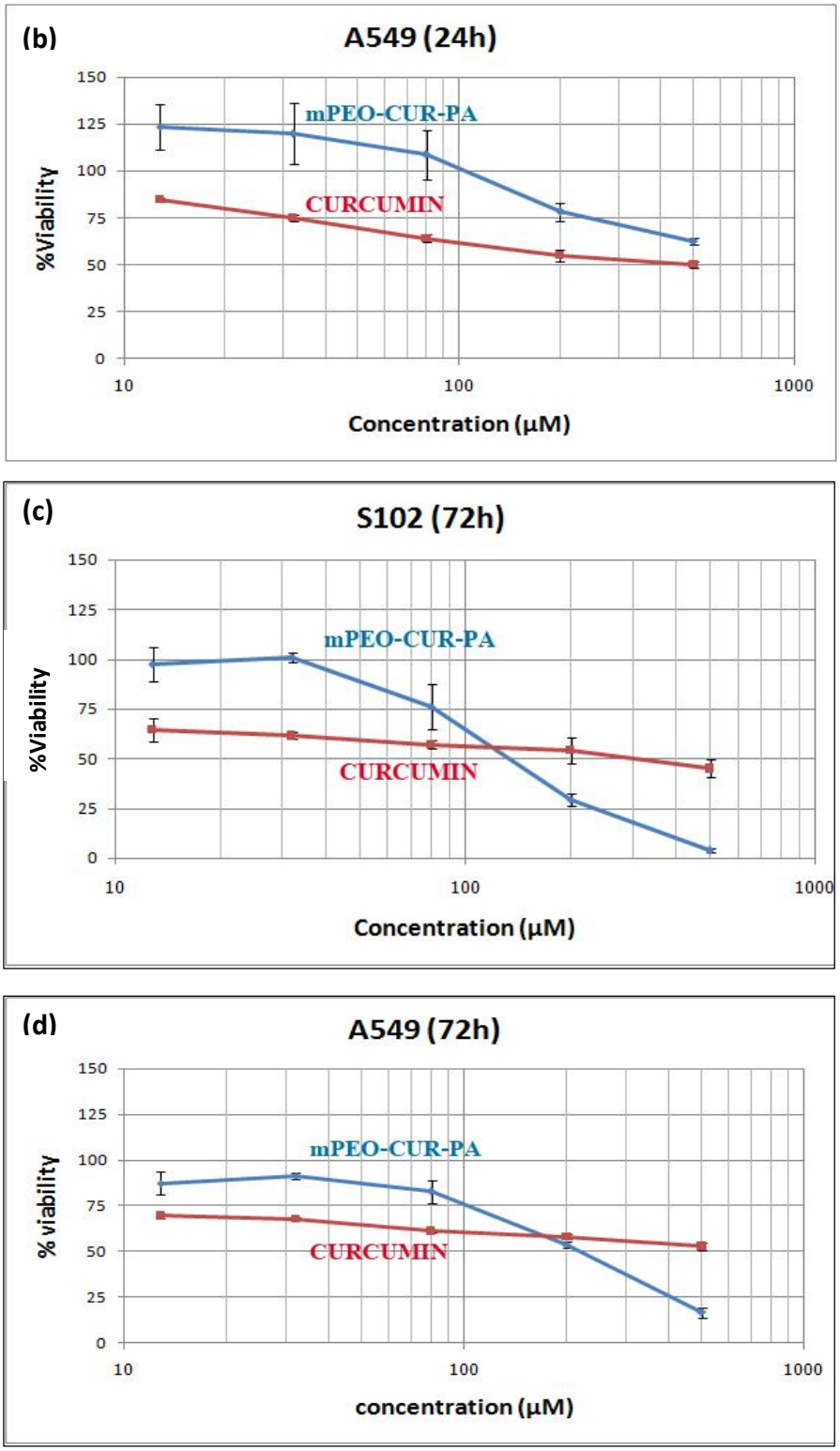

Figure 3.14. Anti-tumor activity of mPEO-CUR-PA and curcumin in S102 and A549 cancer cells. The %viability was showed in (a) S102, (b) A549 at 24 h and (c) S102, (d) A549 at 72 h.

3.6.2 Cellular uptake of mPEO-CUR-PA

To clarify the point on the better cellular uptake of mPEO-CUR-PA in the microspherical form. The uptake of the mPEO-CUR-PA microspheres was studied using HEp-2 human laryngeal carcinoma cells. the sample (100 μM mPEO-CUR-PA (concentration well above the CMC value)) was incubated with HEp-2 cells for 2 h, then stained with acridine orange, and the cells were subjected to confocal fluorescent microscopic analysis which correct the fluorescent signals from 420–750 nm. The fluorescence pictures of the cells were unmixed into mPEO-CUR-PA and acridine orange components, using chemometric analysis (image algorithms) based on the spectral database constructed from fluorescent spectra of standard mPEO-CUR-PA and acridine orange stained on the HEp-2 cells. The fluorescent signal of mPEO-CUR-PA could be clearly detected inside the cells (likely in the lysosomes located in thecytoplasm) (Figure 3.15), indicating that the mPEO-CUR-PA was taken up by the cells. The cellular uptake was likely to occur *via* endocytocis, since spherical morphology of the mPEO-CUR-PA was clearly observed in cytoplasm of the cells. This endocytosis evidence clearly explains the situation in which the anti-tumor activity of mPEO-CUR-PA started to increase at approximately the concentration above the CMC value of the material.

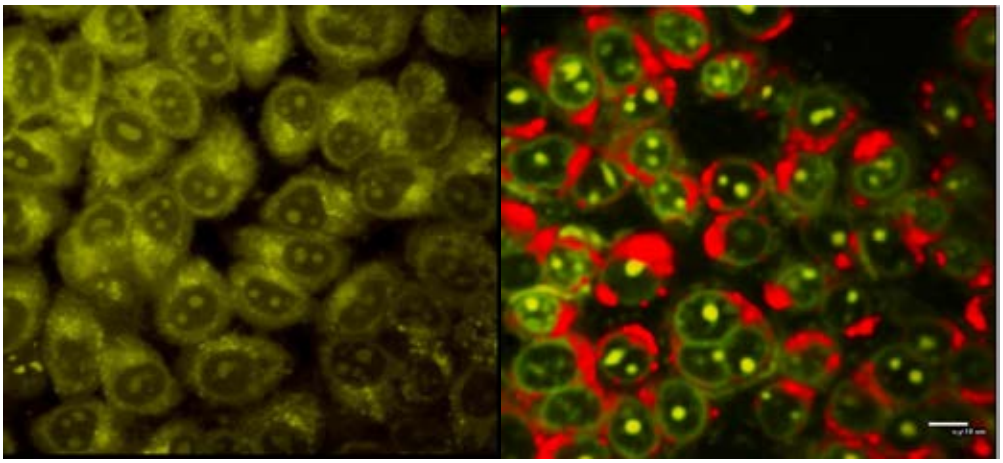

Figure 3.15 The confocal fluorescent pictures; (a) HEp-2 cells stained with acridine orange dye and (b) HEp-2 cells incubated with paclitaxel loaded mPEO-CUR-PA for 2 h and stained with acridine orange. Fluorescence of mPEO-CUR-PA is displayed in red, and that of acridine orange is shown in green.

3.6.3 Cytotoxicity test of paclitaxel loaded mPEO-CUR-PA microspheres

The problem on water solubility of paclitaxel is well recognized [48-50]. Here the effect of vehicle on anti-tumor activity of paclitaxel was also demonstrated, even at very low concentrations of paclitaxel (0.00001 – 0.001 μM). The anti-tumor activity of paclitaxel in culture media containing no DMSO was approximately 30-40% lower than in culture media containing 0.2% DMSO (Figure 3.16). Therefore, to enable the use of paclitaxel in aqueous media, and also to maximize the synergism between curcumin and paclitaxel in killing cancer cells, paclitaxel was loaded into the mPEO-CUR-PA spheres.

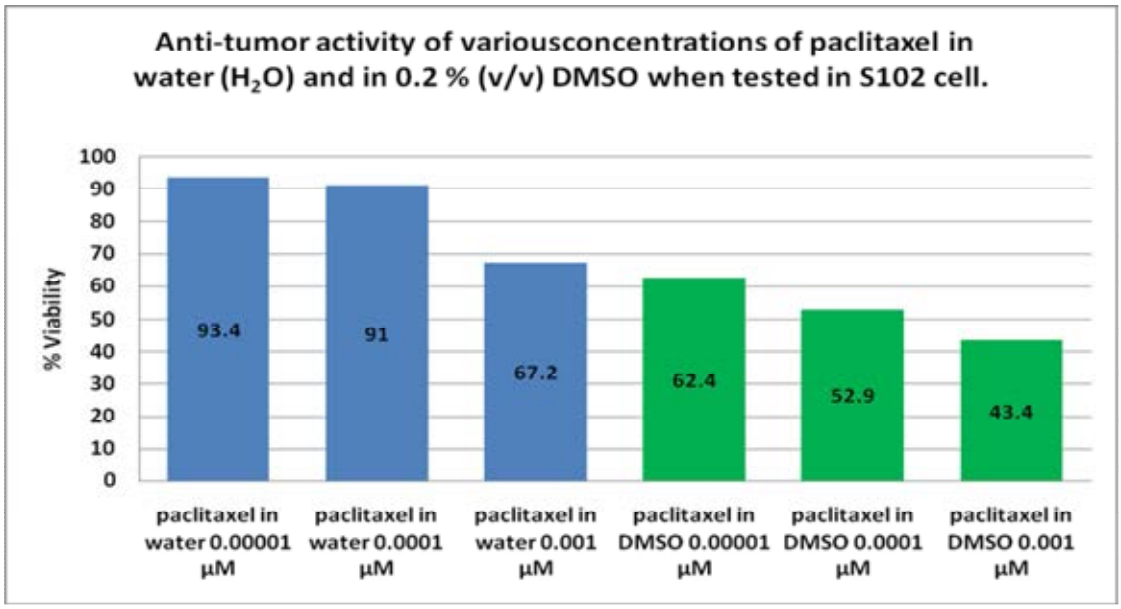

Figure 3.16 Anti-tumor activities of various concentrations of paclitaxel in water (H_2O) and in 0.2 % (v/v) DMSO when tested in S102 cell.

Anti-tumor test of paclitaxel loaded mPEO-CUR-PA microspheres in S102 and A549 cells lines are shown in Figure 3.17(a-c). Significantly higher anti-tumor activity was observed when the mPEO-CUR-PA carriers were used to deliver paclitaxel. Enhancement of the anti-tumor activity of paclitaxel-loaded mPEO-CUR-PA microspheres compared with free paclitaxel in 0.2% DMSO was clearly demonstrated in both S102 and A549 cells; in S102 cells (Figure 3.17 (a)), the %

viability decreased from 102.8% (observed with 0.001 μM free paclitaxel in DMSO) to 54.1% (observed with 0.001 μM encapsulated paclitaxel) and 85.1% (observed with 0.01 μM free paclitaxel in DMSO) to 25.2% (observed with 0.01 μM encapsulated paclitaxel). In A549 cells (Figure 3.17(b)), the %viability also decreased from 93.8% to 35.4% and 51.3% to 16.8% when the mPEO-CUR-PA carriers were used to deliver 0.01μM and 0.1 μM paclitaxel respectively. This clearly indicated the synergism between the carriers and the loaded drug. Since the anti-tumor activity was higher than the use of DMSO as vehicle for paclitaxel, the enhancement was more than just the diminishing of the poor water solubility of paclitaxel. The big improvement is likely a result of i) effective transportation of both drugs (paclitaxel and curcumin derivative) into the cells *via* endocytosis and ii) synergistic effect between paclitaxel and curcumin in killing cancer cells.

Curcumin can overcome drug resistance in cancer cells by blocking drug efflux in multidrug resistant cancer cells [27-28], and can improve anti-cancer activity of paclitaxel by suppressing activation of NF-κB and Akt survival signals induced by paclitaxel [29-30]. Therefore, a paclitaxel-resistant cancer cell, A549RT-eto, was used to test the drug-resistant overcoming efficiency of the paclitaxel-loaded mPEO-CUR-PA. The results showed that drug resistance of the cancer cells could be overcome by the use of paclitaxel-loaded mPEO-CUR-PA. The % viability of 0.01 μM and 0.1 μM paclitaxel treated A549RT-eto cells decreased from 99.5% to 55.9% and from 80.9% to 32.1%, respectively, when the drug was administered through the carriers compared with the use of unencapsulated paclitaxel in DMSO (Figure 3.17 (c)). The synergism between curcumin and paclitaxel is made possible through an ability to effectively co-deliver both paclitaxel and curcumin into the same cells at the same time, thus curcumin is readily available to perform the inhibition on the paclitaxel-resistant mechanism of the cells

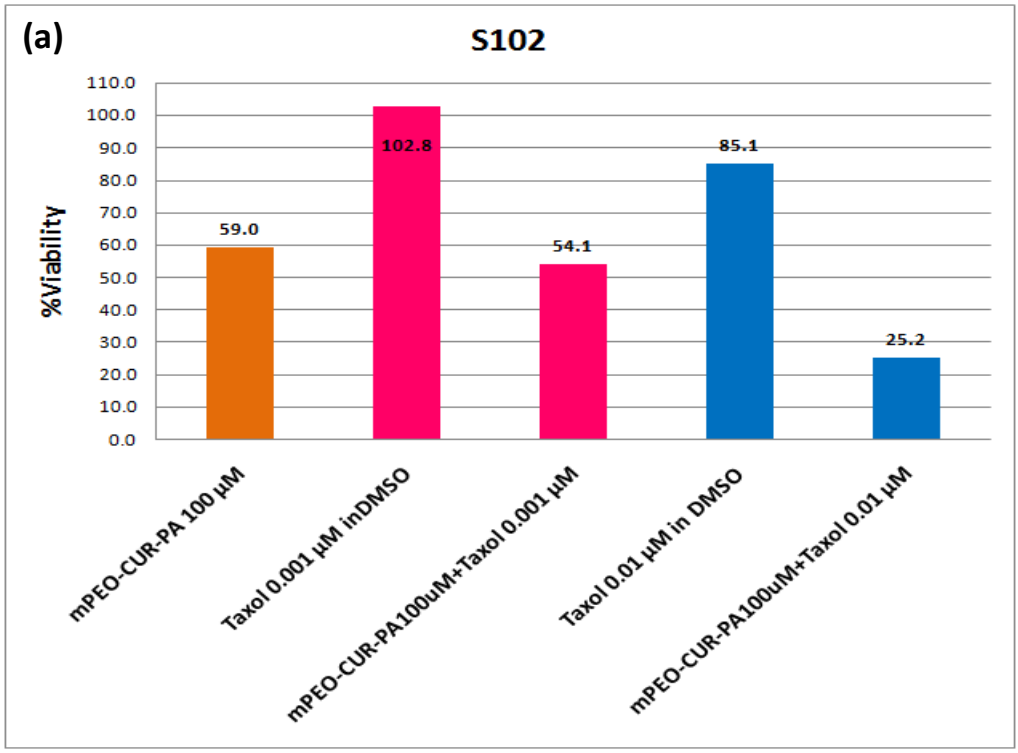
(a)
S102
%Viability
110.0
100.0
90.0
80.0
70.0
60.0
50.0
40.0
30.0
20.0
10.0
0.0
59.0
102.8
54.1
85.1
25.2
mPEO-CUR-PA 100 μM
Taxol 0.001 μM inDMSO
mPEO-CUR-PA100uM+Taxol 0.001 μM
Taxol 0.01 μM in DMSO
mPEO-CUR-PA100uM+Taxol 0.01 μM

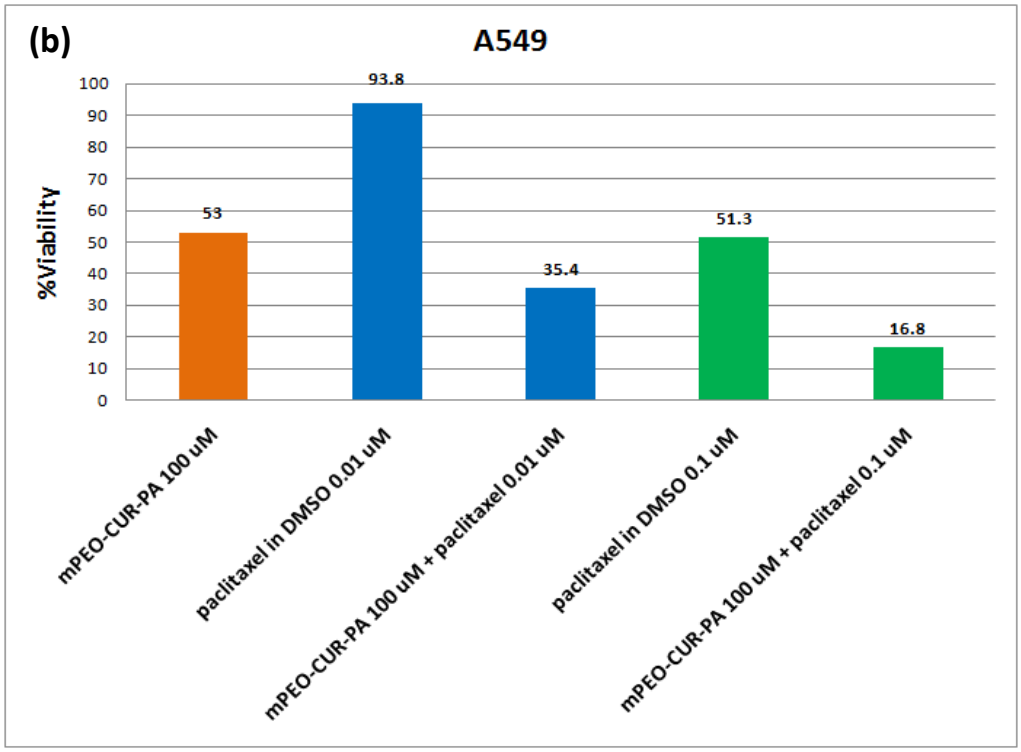
(b)
A549
%Viability
100
90
80
70
60
50
40
30
20
10
0
53
93.8
35.4
51.3
16.8
mPEO-CUR-PA 100 uM
paclitaxel in DMSO 0.01 uM
mPEO-CUR-PA 100 uM + paclitaxel 0.01 uM
paclitaxel in DMSO 0.1 uM
mPEO-CUR-PA 100 uM + paclitaxel 0.1 uM

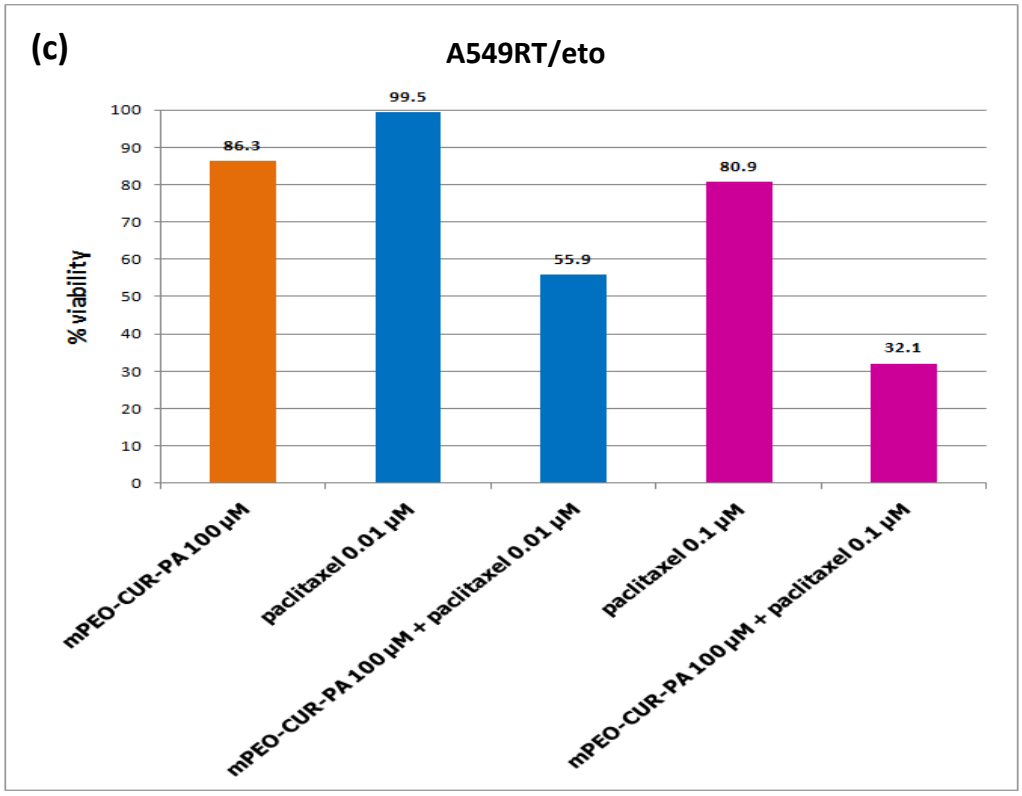

Figure 3.17 Anti-tumor activity of paclitaxel loaded in the mPEO-CUR-PA microspheres comparing with free paclitaxel in 0.2% DMSO and unloaded mPEO-CUR-PA microspheres in (a) S102 cells, (b) A549 cells and (c) A549RT/eto cells.

CHAPTER IV

CONCLUSION

We have successfully synthesized the amphiphillic mPEO-CUR-PA molecule (Figure 4.1) which in water automatically self-assembled into ~ 1.8 μm size spheres at the concentrations above 20 μM which is the CMC value of the material. At the concentrations well above the CMC, the mPEO-CUR-PA showed clear ability to be rapidly taken up by cancer cells via endocytosis. The test of mPEO-CUR-PA in S102 and A549 cells demonstrated better anti-tumor activity than the standard curcumin. Paclitaxel was successfully loaded into the mPEO-CUR-PA microspheres. Enhancement in anti-tumor activity of the paclitaxel-loaded mPEO-CUR-PA microspheres was observed in both of S102 and A549 cell. In S102 cells, up to 48% and 60% enhancements were witnessed when the 0.001 and 0.01 μM paclitaxel were used in the mPEO-CUR-PA encapsulated form comparing to that used as unencapsulated drug in DMSO, respectively. In A549 cells, up to 59% and 34% enhancements were observed at the paclitaxel concentration of 0.01 and 0.1 μM, respectively. These indicates synergism between paclitaxel and curcumin. The use of mPEO-CUR-PA carrier to deliver paclitaxel into paclitaxel-resistant cancer cells resulted in overcoming drug resistance of the cells. In paclitaxel-resistant cancer cells (A549RT-eto), the enhancements of 43% and 48% were observed at 0.01 and 0.1 μM free paclitaxel, respectively. This demonstration of bioactive carrier that works synergistically with the loaded drug should open up the possibility to not only use lower concentration of paclitaxel but also overcome the drug resistance in cancer treatment. Other combination of drugs can also be explored.

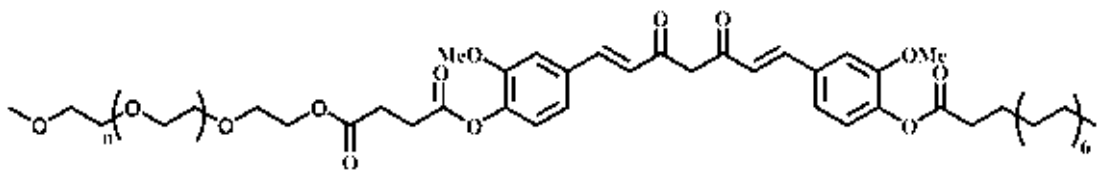

Figure 4.1 Structure of mPEO-CUR-PA molecule

References

[1] Malmsten, M.; Lindman, B. *Macromolecules* **1992**, *25*, 5440.

[2] Allen, T.M.; Cullis, P.R. *Drug Discovery* **2004**, *303*, 1818.

[3] Kataoka, K.; Kwon G. S.; Yokoyama M.; Okano, T.; Sakurai Y. *Journal of controlled release* **1993**, *24*, 119.

[4] Uhrich, K. E.; Cannizzaro, S. M.; Langer, R. S.; Shakesheff, K. M. *Chemical Reviews* **1999**, *99*, 3181.

[5] Shen, Y.; Jin, E.; Zhang, B.; Murphy, C. J.; Sui, M.; Zhao, J.; Wang, J.; Tang, J.; Fan, M.; Van Kirk, E.; Murdoch, W. J. *Journal of the American Chemical Society* **2010**, *132*, 4259.

[6] Anumansirikul, N.; Wittayasuporn, M.; Klinubol, P.; Tachaprutinun, A.; Wanichwecharungruang, S. P. *Nanotechnology* **2008**, 205101, *9pp.*

[7] Kidsaneepoiboon, P.; Wanichwecharungruang, S. P.; Chooppawa, T.; Deephum, R.; Panyathanmaporn, T. *Journal of Materials Chemistry* **2011**, *21*, 7922.

[8] Maeda, H.; Matsumura, Y. *Crit. Rev. Ther. Drug Carrier Sys.* **1989**, *6*, 193–210.

[9] Maeda, H. *Advanced Drug Delivery Reviews* **1991**, *6*, 181.

[10] Maeda, H. *Polymer Site Specific Pharmacotherapy* (Domb, A. J. ed.), Wiley: New York, USA **1994**, *95pp.*

[11] Madea, H.; Seymour, L.; Miyamoto, Y. *Bioconjugate Chemistry* **1992**, *3*, 351.

[12] Iwai, K.; Maedea, H.; Konno, T.; *Cancer Research* **1984**, *44*, 2115.

[13] Noguchi, Y. Wu, J.; Duncan, R.; Strohalm, J.; Ulbrich, K.; Akaike, T.; Maede, H. *Japanese Journal of Cancer Research* **1998**, *89*, 307.

[14] Iwai, K.; Maeda, H.; Konno, T.; Matshunura, Y.; Yamashita, R.; Yamasaki, K.; Hirayama, S.; Miyauchi, Y. *Anticancer Research* **1987**, *7*,321.

[15] Maeda, H.; Matsumoto, T.; Konno, T.; Iwai, K.; Ueda, M. *Journal of Protein Chemistry* **1984**, *3*, 181.

[16] Maeda, H.; Matsumura, Y.; Oda, T.; Sasamoto, K. *Protein Tailoring for Food and Medical Uses* (Feeney, R. E.; Whitaker, J. R. eds.), Marcel Dekker Inc.: New York, USA **1986**, *353 pp.*

[17] Hatcher, H.; Planalp, R.; Cho, J.; Torti, F. M.; Torti, S. V. *Cellular and Molecular Life Sciences* **2008**, *65*, 1631.

[18] Washington, N.; Washington, C.; Wilson, C. G. *Physiological pharmaceutics: Barriers to drug absorption* (Washington, N. ed.), Taylor and Francis: London **2001**, *181pp.*

[19] Anand, P.; Kunnumakkara, A. B.; Newman, R. A. *Molecular Pharmaceutics* **2007**, *4*, 807.

[20] Shishodia, S.; Sethi, G.; Aggarwal, B. B. *Annals of the New York Academy of Sciences* **2005**, *1056* (1): 206.

[21] Cheng, A.L.; Hsu, C.H.; LIN, J.K.; Hsu, M.M.; Ho, Y.F.; Shen, T.S.; Ko, J.Y.; Lin, J.T.; Lin, B.R.; Ming-Shiang, W.; Yu, H.S.; Jee, S.H.; Chen, G.S.; Chen, T.M.; Chen, C.A.; Lai, M.K.; Pu, Y.S.; Pan, M.H.; Wang, Y.J.; Tsai, C.C.; Hsieh, C.Y. *Anticancer Research* **2001**, *21*, 2895.

[22] Bharat, B.A.; Anushree, K.; Alok, C.B. *Anticancer research* **2003**, *23*, 363.

[23] Yang, F.; Begum, A. *Neurobiology of Aging* **2004**, *25*, 158.

[24] Ruby, A.J.; Kuttan, G.; Babu, K.D.; Rajasekharan, K.N.; Kuttan, R. *Cancer Letters* **1995**, *94* , 79.

[25] Lantz, R.C.; Chen, G.J.; Solyom, A.M.; Jolad, S.D.; Timmermann, B.N. *Phytomedicine* **2005**, *12*, 445.

[26] Abe, Y.; Hashimoto, S.; Horie, T. *Pharmacological Research* **1999**, *39*, 41.

[27] Limtrakul, P.; Chearwae, W.; Shukla, S.; Phisalphong, C.; Ambudkar, S. V. *Molecular and cellular biochemistry* **2007**, *296*, 85.

[28] Chearwae, W.; Wu, C. P.; Chu, H. Y.; Lee, T. R.; Ambudkar, S. V.; Limtrakul, P. *Cancer chemotherapy and pharmacology* **2006**, *57*, 376.

[29] Bava, S. V.; Puliappadamba, V. T.; Deepti, A.; Nair, A.; Karunagaran, D.; Anto, R. J. *Journal of Biological Chemistry* **2005**, *280*, 6301.

[30] Bava, S. V.; Sreekanth, C. N.; Thulasidasan, A. K. T.; Anto, N. P.; Cheriyan, V. T.; Puliyappadamba, V. T.; Menon, S. G.; Ravichandran, S. D.; Anto, R. J. *International Journal of Biochemistry and Cell Biology* **2011**, *43*, 331.

[31] Shishodia, S.; Amin, H. M.; Lai, R.; Aggarwal, B. B. *Biochemical Pharmacology* **2005**, *70*, 700.

[32] Aggarwal, B. B.; Shishodia, S.; Takada, Y.; Banerjee, S.; Newman, R. A.; Bueso-Ramos, C. E.; Price, J. E. *Clinical Cancer Research* **2005**, *11*, 7490.

[33] Siwak, D. R.; Shishodia, S.; Aggarwal, B. B.; Kurzrock, R. *Cancer* **2005**, *104*, 879.

[34] Aziz, H. A.; Peh, K. K.; Tan, Y. T. F. *Drug Development and Industrial Pharmacy* **2007**, *33*, 1263.

[35] Bisht, S.; Feldmann, G.; Soni, S.; Ravi, R.; Karikar, C.; Maitra, A.; Maitra, A. *Journal of Nanobiotechnology* **2007**, *5*(3), *18pp.*

[36] Sahu, A.; Bora, U.; Kasoju, N.; Goswami, P. *Acta Biomaterialia* **2008**, *4*, 1752.

[37] Cui, J.; Yu, B.; Zhao, Y.; Zhu, W.; Li, H.; Lou, H.; Zhai, G. *International Journal of Pharmaceutics* **2009**, *371*,148.

[38] Shaikh, J.; Ankola, D. D.; Beniwal, V.; Singh, D.; Kumar, M. N. *European Journal of Pharmaceutical Sciences* 2009, *37*, 223.

[39] Das, R. K.; Kasoju, N.; Bora, U. *Journal of Nanomedicine* **2010**, *6*, 153.

[40] Anand, P.; Nair, H.B.; Sung, B.; Kunnumakkara, A.B.; Yadav, V.R.; Tekmal, R.R.; Aggarwal, B.B. *Biochemical* Pharmacology 2010, *79*, 330.

[41] Yen, F. L.; Wu, T. H.; Tzeng, C. W.; Lin. L. T.; Lin. C. C. *Journal of Agricultural and Food Chemistry* **2010**, *58*, 7376.

[42] Kumar, S.; Dubey, K. K.; Tripathi, S.; Fujii, M.; Misra, K.; *Nucleic Acids Symposium Series* **2000**, *44*, 75.

[43] Mohri, K.; Watanabe, Y.; Yoshida, Y.; Satoh, M.;Isobe, K.; Sukimoto, N.; Tsuda, Y.; *Chemical & Pharmaceutical Bulletin* **2003**, *51*(11), 1268.

[44] Venkateswarlu, M.; Ramachandra, S.; Subbaraju, G. V. *Bioorganic & Medicinal Chemistry* **2005**, *13*, 6374.

[45] Safavy, A.; Raisch, K.P.; Mantena, S.; Sanford, L.L.; Sham, S.W.; Krishna, N.R.; Bonner, J.A. *Journal of Medicinal Chemistry* **2007**, 50, 6284.

[46] Tang, H.; Murphy, C.J.; Zhang, B.; Shen, Y.; Krik, E.A.V.; Murdoch, W.J.; Radosz. Biomaterials **2010**, *31*, 7139.

[47] Manju, S.; Sreenivasan, K. *Journal of Colloid and Interface Science* **2011**, *359*, 318.

[48] Huh, K.M.; Lee, S.C.; Cho, Y.W.; Lee, J.; Jeong, J.H.; Park, K. *Journal of Controlled Release* **2005**, *101*, 59.

[49] Mugabe, C.; Hadaschik, B.A.; Kainthan, R.K.; Brooks, D.E.; So, A.I.; Gleave, M.E.; Burt, H.M. *Journal compilation© 2 0 0 8 BJU International* **2008**, *103*, 978.

[50] Bava, S.V.; Puliappadamba, V.T.; Deepti, A.; Nair, A.; Karunagaran, d.; Anto, R.J. *The Journal of biological chemistry* **2005**, *280*(8), 6301.

[51] Laohathai, K.; Bhamarapravati, N. *American Journal of Pathology* **1985**, *118*, 203.

[52] Kanintronkul, Y.; Worayuthakarn, R.; Thasana, N.; Winayanuwattikun, R.; Pattanapanyasat, K.; Surarit, R.; Ruchirawat, S.; Svasti, J. *Anticancer Research* **2011**, *31*, 921.

[53] Suwannateep, N.; Banlunara, W.; Wanichwecharungruang, S. P.; Chiablaem, K.; Lirdprapamongkol, K.; Svasti, J. *Journal of Controlled Release* **2011**, *151*, 176.

VITAE

Miss. Kittima Chondejchartwut was born on April 23, 1987 in Bankok, Thailand. She received a Bachelor's Degree of Science in Chemistry from Chulalongkorn University in 2008. And then, she started her graduate study a Master's degree in the Program of Chemistry, Faculty of Science, Chulalongkorn University. During master study, she had a great opportunity to presented her work in poster session in the topic of "Synthesis and development of curcumin derivatives as anticancer agents" at the 7th International Symposium on Advanced Materials in Asia-Pacific (7th ISAMAP). The finance for joining the conference was supported by National Center of Excellence for Petroleum, Petrochemicals and Advanced Materials (NCE-PPAM) and the Graduate School, Chulalongkorn University.

Her present address is 939/17 Klongjan, Bangkapi, Bangkok Thailand 10240.